Leveraging 3D printing to enhance mass spectrometry

Grajewski, M.; Hermann, M.; Oleschuk, R. D.; Verpoorte, E.; Salentijn, G. Ij.

Published in:
Analytica Chimica Acta

DOI:
10.1016/j.aca.2021.338332

Publication date:
2021

Analytica Chimica Acta 1166 (2021) 338332

Contents lists available at ScienceDirect

Analytica Chimica Acta

journal homepage: www.elsevier.com/locate/aca

Leveraging 3D printing to enhance mass spectrometry: A review

M. Grajewski [a], M. Hermann [b], R.D. Oleschuk [b], E. Verpoorte [a], G.IJ. Salentijn [c, d, *]

[a] Pharmaceutical Analysis, Groningen Research Institute of Pharmacy, University of Groningen, Groningen, the Netherlands
[b] Department of Chemistry, Queen's University, Kingston, Ontario, Canada
[c] Wageningen Food Safety Research (WFSR), Wageningen University & Research, Wageningen, the Netherlands
[d] Laboratory of Organic Chemistry, Wageningen University, Wageningen, the Netherlands

HIGHLIGHTS

- Overview, strengths and limitations of 3D printers and materials for mass spectrometry.
- Comprehensive review of 3D printing for enhancing mass spectrometry from 2013 to 2020.
- Critical analysis of how 3D printing has and further can innovate mass spectrometry.

GRAPHICAL ABSTRACT

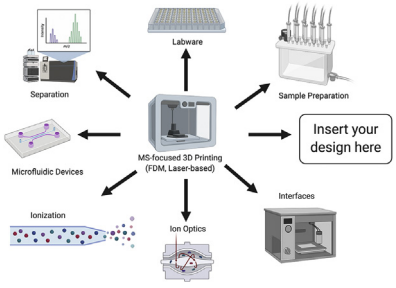

ARTICLE INFO

Article history:
Received 31 December 2020
Received in revised form
12 February 2021
Accepted 15 February 2021
Available online 23 February 2021

Keywords:
Rapid prototyping
Stereolithography
Fused-deposition modelling
Ambient ionization
Ion transport
Sample preparation

ABSTRACT

The use of 3D printing in the chemical and analytical sciences has gained a lot of momentum in recent years. Some of the earliest publications detailed 3D-printed interfaces for mass spectrometry, which is an evolving family of powerful detection techniques. Since then, the application of 3D printing for enhancing mass spectrometry has significantly diversified, with important reasons for its application including flexible integration of different parts or devices, fast customization of setups, additional functionality, portability, cost-effectiveness, and user-friendliness. Moreover, computer-aided design (CAD) and 3D printing enables the rapid and wide distribution of scientific and engineering knowledge. 3D printers allow fast prototyping with constantly increasing resolution in a broad range of materials using different fabrication principles. Moreover, 3D printing has proven its value in the development of novel technologies for multiple analytical applications such as online and offline sample preparation, ionization, ion transport, and developing interfaces for the mass spectrometer. Additionally, 3D-printed devices are often used for the protection of more fragile elements of a sample preparation system in a customized fashion, and allow the embedding of external components into an integrated system for mass spectrometric analysis. This review comprehensively addresses these developments, since their introduction in 2013. Moreover, the challenges and choices with respect to the selection of the most appropriate printing process in combination with an appropriate material for a mass spectrometric application are addressed; special attention is paid to chemical compatibility, ease of production, and cost. In this review, we critically discuss these developments and assess their impact on mass spectrometry.

* Corresponding author. Wageningen Food Safety Research (WFSR), Wageningen University & Research, P.O. Box 230, 6700, AE, Wageningen, the Netherlands.
E-mail address: gert.salentijn@wur.nl (G.IJ. Salentijn).

https://doi.org/10.1016/j.aca.2021.338332

Contents

1. Introduction 2
2. Materials and printing processes for mass spectrometry 3
   2.1. Fused-deposition modelling 4
      2.1.1. Polylactic acid (PLA) 4
      2.1.2. Acrylonitrile butadiene styrene (ABS) 4
      2.1.3. Polypropylene (PP) 5
      2.1.4. Polyether-ether-ketone (PEEK) 5
      2.1.5. Functionalized FDM materials 5
   2.2. Laser-based 3D printing 5
      2.2.1. Stereolithography 5
      2.2.2. Polyjet 6
      2.2.3. Selective laser sintering 6
3. Applications of 3D printing for mass spectrometry 6
   3.1. Sample preparation 6
      3.1.1. Offline sample preparation 6
      3.1.2. Online sample preparation 9
   3.2. Ion introduction 9
      3.2.1. Ionization 9
      3.2.2. Ion guides 11
   3.3. Platforms 13
      3.3.1. MS interfaces 13
      3.3.2. Housing and integration 14
4. Conclusion and future directions 14
   CRediT authorship contribution statement 15
   Declaration of competing interest 15
   Acknowledgements 15
   References 15

Abbreviations

ABS	Acrylonitrile butadiene styrene
AIMS	Ambient ionization mass spectrometry
CAD	Computer-aided design
CE	Capillary electrophoresis
C^4D	Capacitively coupled contactless conductivity detector
DART	Direct analysis in real time
DESI	Desorption electrospray ionization
DIY	Do-it-yourself
DoA	Drugs of abuse
(nano)ESI	(nano) Electrospray ionization
FDM	Fused-deposition modelling
FT-ICR	Fourier transform ion cyclotron resonance
GC	Gas chromatography
ICP	Inductively coupled plasma
HPLC	High-pressure liquid chromatography
HIPS	High-impact polystyrene
IMS	Ion mobility spectrometry
LIT	Linear ion trap
LMJSSP	Liquid micro-junction surface-sampling probe
LPME	Liquid-phase microextraction
LSAP-GD	Liquid-sampling atmospheric-pressure glow discharge
LTP	Low-temperature plasma
MALDI	Matrix-assisted laser desorption ionization
MS	Mass spectrometry/mass spectrometer
MS/MS	Tandem mass spectrometry
PA	Polyamide
PC	Polycarbonate
PEEK	Polyether-ether-ketone
PET(G)	Polyethylene terephthalate (glycol)
PHA	Polyhydroxyalkanoate
PLA	Polylactic acid
PP	Polypropylene
PS	Paper spray
PVA	Polyvinyl acid
Q	Quadrupole
QqQ	Triple quadrupole
SLA	Stereolithography
SLS	Selective laser sintering
SPE	Solid-phase extraction
TOF	Time-of-flight
V-EASI	Venturi easy ambient sonic-spray ionization
3D-IT	Three-dimensional ion trap

1. Introduction

In this review, innovation through 3D printing for mass spectrometry (MS) and its future potential are critically assessed. 3D printing has become quite popular in many scientific areas, as it allows the rapid design and fabrication of experimental tools and components for analytical instrumentation. The 3D design of these parts is accomplished with computer-aided design (CAD) software.

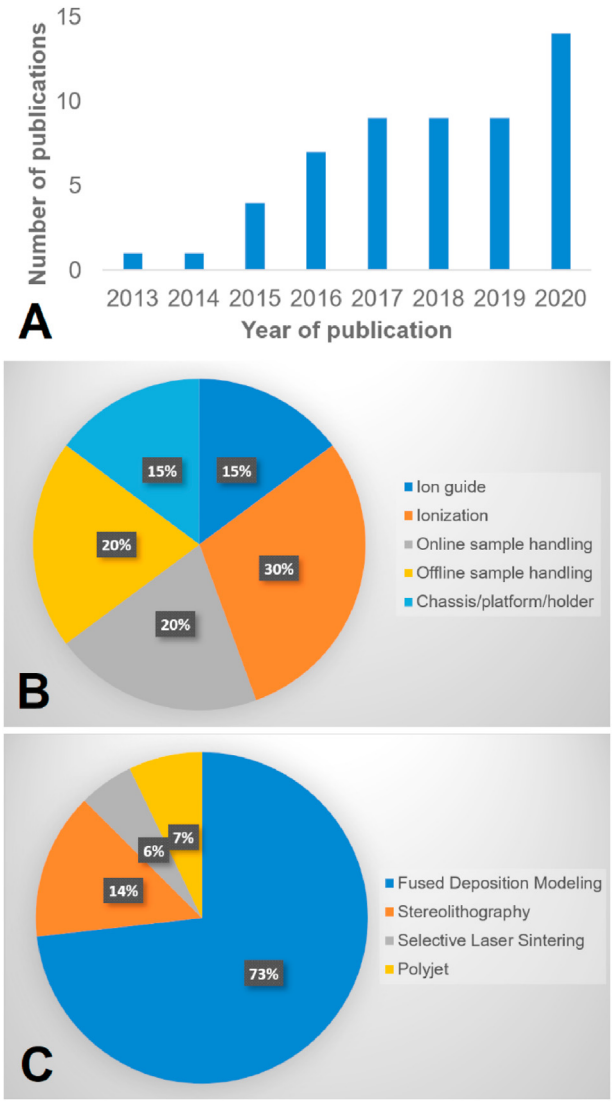

Fig. 1. Overview of the use of 3D printing to enhance mass spectrometry. (A) Number of publications per year on the topic. (B) Classification of these publications based upon their function, and (C) the type of printer used for their production.

After drawing, designs can be simply processed with freeware (conversion to *stl file, and slicing of the model) in preparation for production in a wide range of plastics and other materials. Mass spectrometry is also an area of great scientific interest, as it allows the separation and detection of charged species based on their mass-to-charge ratio. The method is crucial to analytical workflows including proteomics, metabolomics, but also for structure elucidation, food safety, (bio)medical analysis, and chemical imaging.

The combination of MS with 3D printing might not be immediately obvious, and yet at the same time, it makes a lot of sense. On the one hand, there is MS, one of the most versatile technologies in the modern arsenal of analytical instrumentation, characterized by (i) high acquisition and maintenance costs, (ii) unsurpassed analytical performance, (iii) general applicability (though certainly not always) as a 'black box' in an analytical workflow, and (iv) usage predominantly in a lab-based setting (though portable MS is on the rise [1]). On the other hand, 3D printing is also a versatile technology, but unlike MS, is characterized by: (i) low acquisition and material costs, (ii) variable and often limited resolution and reproducibility, (iii) easy interaction with, and operation by, users, (iv) an open-source technology which is highly dispersed and available globally. The obvious question resulting from their paradoxical nature is 'How can cost-effective, simple, customizable 3D-printed parts, of not always the highest quality or best material, be leveraged to enhance such a powerful, highly-optimized and less accessible technology like MS?' Despite the advantages of MS, most scientists consider MS instrumentation to be big, bulky, highly refined and non-customizable black boxes. However, research applications often require the opposite, namely the potential to tailor a setup to an experiment or workflow. 3D printing allows one to combine the best of both worlds, mating rapid prototyping and sample introduction customization with dependable detection schemes. 3D printing does not always result in a perfectly fabricated part, made from a material with the most suitable properties, but it does allow one to quickly develop and test potential solutions for urgent research-limiting issues.

Moreover, sharing of CAD files and 3D models, which can then be quickly printed all around the world, will facilitate the distribution of these approaches and the democratization of mass spectrometry. This review covers different aspects of the marriage between 3D printing and MS, namely the reasons why it works (interfacing possibilities, integration, additional functionality), and challenges (material selection, limitation of material properties, printability).

For this review, the search term [*mass* AND *spectrometry* AND *3D* AND *printing*] was used in the Web of Science. Papers were selected based upon the title, abstract and keywords when they met the following requirements: (i) an application of 3D printing was described, and (ii) the application was in service of MS analysis (rather than using MS to characterize a 3D-printed device), or at least demonstrating clear applicability to MS. The number of papers describing the application of 3D printing to enhance MS were plotted per year of publication (Fig. 1A) and grouped into different categories based on their function (Fig. 1B), and the type of 3D printing used (Fig. 1C). The different printing processes encountered in these publications are described and assessed, as well as the different materials that are most frequently used in these instances. In the second part of the review, a comprehensive overview of the applications of 3D printing for MS is given. These applications are listed in Tables 2–6, along with information on the purpose of 3D printing, the type of mass spectrometer and interface, the printing technique and materials used, and tested solutions or applications.

2. Materials and printing processes for mass spectrometry

There are many issues to consider when opting for 3D printing in the analytical sciences, and these are mainly related to the available materials and different printing processes. Compatibility between the material and solvents used, as well as other, external factors set by the researchers, such as elevated temperatures (i.e. to promote desolvation), are limiting factors in MS. For example, when using a 3D-printed device for the extraction of trace components from a complex sample, it would be detrimental if the eluent also extracted compounds from the printed part that could lead to ion suppression. At the same time, surface coatings and modification strategies might be employed to mitigate these problems to a certain extent. Moreover, the preferred material may not always be the easiest material to print with, due to its melting temperature, for example. In this section, four printing processes that are commonly used for MS applications (see Fig. 1C), namely Fused-Deposition Modelling (FDM), Stereolithography (SLA), PolyJet, and Selective Laser Sintering (SLS) printing, are discussed, as well as the materials encountered in these processes (see Table 1).

Table 1
3D printing technologies and materials for MS.

Technology	Material	Strengths	Limitations
FDM		- Very cost-effective - Wide range of materials	- Thermoplastics usually have low thermal resistance - High degree of anisotropy - Typically no water/airtightness without post-processing - Minimum XY resolution limited to around 150 μm
	PLA	- Easy to print (high-temperature tolerance, low/no warping, very popular) - Cost-effective - Biocompatible - Environmentally friendly	- Weak mechanical properties - Low thermal stability - Limited chemical resistance
	ABS	- Easy to print (high-temperature tolerance, low/no warping, very popular) - Good mechanical properties	- Low thermal stability - Limited chemical resistance
	PP	- Superior chemical resistance - Better thermal stability than PLA and ABS	- Semi-crystalline and prone to warping - Low adhesion to common printing bed surfaces - Weak mechanical properties
	PEEK	- Excellent chemical resistance - Excellent mechanical properties - High thermal stability	- Limited commercial availability and therefore expensive - Requires high processing temperatures and custom FDM printer
SLA		- Low-cost technology - Good air and water tightness - Smooth surface finish (laminar flow when used in microfluidic devices) - Good resolution (XY around 50 μm, Z around 10 μm) - Good mechanical stability	- Usually low/no biocompatibility due to residual initiator and monomers
	Silica Glass	- Outstanding thermal stability - Outstanding chemical resistance - Good optical transparency - Excellent mechanical properties	- Not commercially available
SLS		- High control over porosity - Materials that are not printable by common 3D printing techniques (metals, ceramics) - Good resolution (XY around 50 μm, Z around 10 μm)	- High acquisition costs
PolyJet		- Multi-material capability with polymers that have a wide variety of properties - Good air and water tightness - Smooth surface finish - High resolution (XYZ around 15 μm)	- Very high acquisition and consumable costs

2.1. Fused-deposition modelling

Fused-deposition modelling is the most accessible printing technology currently available and is based on the melting of thermoplastics in a heated part, from which the molten plastic is extruded through a narrow orifice at the bottom by supplying new filament from the top. This thin extruded thread is deposited onto a platform to produce a layer in any desired shape. By addition of subsequent layers, a 3D part is formed. Some FDM printers have multiple extrusion heads or automated filament-changing compatibility, which allows the printing of different materials in a single part (dual-head printing). The resolution of FDM in the X and Y direction is determined by its nozzle diameter. Most commercially available 3D printers are compatible with nozzle diameters in the range of 150–600 μm, where 400 μm nozzles are the most common ones. The resolution in the Z direction is mostly determined by manufacturing and assembly tolerances and for commercially available printers is typically in the range of 50–150 μm.

2.1.1. Polylactic acid (PLA)

Polylactic acid is one of the most used materials for FDM 3D printing, including MS applications. As an amorphous thermoplastic, it is easy to print, as it experiences low warping, can be printed with reasonable resolution, has a low sensitivity to moisture, and a low tendency to clog the nozzle. With respect to printing temperatures, PLA exhibits a wide range starting at low temperatures (Melting temperature, T_m = 150–170 °C), and is therefore forgiving to temperature fluctuation. This material can therefore be printed on budget FDM 3D printers that do not provide a heated printing bed, a high-temperature-extruder, or an enclosure. PLA has numerous environmental advantages, as it is derived from renewable sources such as rice or corn starch, it is biodegradable and recyclable [2,3], and its production fixates carbon dioxide [4]. Due to its biocompatibility, PLA is used clinically for implants, in theranostics, and drug delivery systems [5–7]. A drawback of PLA is its brittleness and therefore poor toughness [8,9]. The low melting and glass transition temperature (T_g = 60–70 °C) make processing PLA easy, but this leads to low thermal stability [10]. Martinez-Jarquin et al. compared the performance of low-temperature plasma probes that were 3D printed with PLA, acrylonitrile butadiene styrene (ABS), and polycarbonate (PC), and report that the probe made of PLA experienced deformation at high voltages due to its low glass transition temperature [11]. 3D-printed PLA shows good physical stability when in contact with water, ethanol, acetic acid, triethylamine, hexane, diethyl ether, and moderate stability with ethyl acetate, toluene, dimethylformamide, and tetrahydrofuran [12,13]. It has a relatively high hydrophobicity, with a water contact angle of 75–85° [14]. Elviri et al. fabricated a desorption electrospray ionization (DESI) substrate made of PLA because of its ease-of-use, insolubility in water, and hydrophobicity [15]. Even though PLA is soluble in acetonitrile [16–19], it was possible to use these DESI substrates with H_2O/ACN (50:50) as the DESI solvent. Furthermore, Salentijn et al. were able to use 3D-printed PLA cartridges that were in direct contact with common ESI-MS solvent mixtures such as H_2O/MeOH (50:50 and 10:90) and H_2O/acetonitrile (50:50) [19], while Jönsson et al. have demonstrated that PLA printed parts can withstand pressures of up to ~46 bar, allowing their use in LC-MS applications [20].

2.1.2. Acrylonitrile butadiene styrene (ABS)

ABS is the second most used material in FDM printing behind PLA [21,22]. Its low glass transition temperature (T_g = 110 °C) and excellent processing properties make it a popular choice in FDM 3D

printing [23–25]. A drawback is that volatile organic compounds such as styrene and ultrafine particles, which are detrimental to health and the environment, are emitted when ABS is printed [26,27]. As an amorphous polymer, ABS experiences low shrinkage and warping during the cooling process and allows fabrication of parts with high accuracy and dimensional stability [28].

3D-printed parts made of ABS have good impact resistance and toughness with tensile strengths ranging from 28.5 to 37.0 MPa, and elastic moduli of 1807–2050 MPa [29–32]. ABS is not widely used in medical devices, because its layers do not blend together well to create water-tight parts, and it is not considered to be biocompatible [33]. To improve biocompatibility and water-tightness of FDM-printed ABS parts, acetone sealing and surface grafting of polyethylene glycol chains have been suggested, which also increases the resistance to non-specific protein adhesion [33]. The solvent resistance of ABS-printed parts have been tested by Gordeev et al. by bringing parts in contact with different solvents for an hour at room temperature. ABS-printed parts have shown good stability with water, hexane, diethyl ether, and ethanol, and no chemical resistance when in contact with acetonitrile, acetone, dimethylsulfoxide, dichloromethane, tetrahydrofuran, and toluene [13]. Duarte et al. tested the solvent permeation resistance of ABS before its usage as a paper cartridge for paper-assisted direct spray ionization MS. Pieces of native ABS filament immersed in water and 0.1% formic acid solution in methanol for 7h hours showed no noticeable changes over time, while exposure to acetone and acetonitrile led to swelling and degradation [34]. Due to its toughness, stability, and ease of printing, ABS has been chosen as a material to print holders in some MS applications [35–37].

2.1.3. Polypropylene (PP)

Polypropylene is not as easy to print as PLA and ABS and is therefore less popular in FDM printing. PP is a semi-crystalline polymer and not amorphous like PLA and ABS. Once the temperature of PP drops below its melting temperature, crystallization starts at the molecular level which leads to contraction and warping [38]. The tendency of PP to warp, together with its low surface tension, leads also to low adhesion of parts to the printing surface. Adhesion to the print bed can be enhanced using a polypropylene sheet or covering the printing bed with a packaging tape made with polypropylene [39,40]. Compared to PLA and ABS, PP shows good thermal stability. Hilton et al. were able to perform addition reactions at 150 °C in columns made of PP [40]. 3D-printed PP parts show good stability when in contact with acetonitrile, water, dimethylsulfoxide, diethyl ether, and ethanol, and moderate stability when in contact with acetone, hexane, dichloromethane, tetrahydrofuran, and toluene [13]. Due to its superior solvent compatibility, PP has been chosen as a material for an online reaction container that is directly connected to a nano-ESI capillary by Scotti et al. [39] This reaction chamber was used to perform a Diels-Alder reaction between *trans*-cyclooctene and methyltetrazine followed by a retro Diels-Alder reaction with acetonitrile/water (80:20) + 0.1% formic acid. Similarly, Mathieson et al. have chosen PP due to its cost-effectiveness, robustness, flexibility, and chemical inertness to print a reaction chamber used for supramolecular coordination reactions that are monitored in real-time by ESI-MS [41]. Sramkova et al. demonstrated the use of 3D-printed stirring devices for solid-phase-extraction (SPE) of bisphenols from water samples [18]. The stirring device holds fibres for semi-dispersive extraction and a stir bar that allows one to spin the device, enabling highly efficient interaction of the sorptive fibres with the analytes. Different materials were tested for 3D printing of the stirring device, where PP was found to be the best suited filament due to its chemical stability and low degree of leaching when immersed in solvents such as ethanol and methanol.

2.1.4. Polyether-ether-ketone (PEEK)

PEEK is a semi-crystalline thermoplastic with good thermal stability (T_m = 343 °C) and high mechanical strength (tensile strength of FDM-printed parts: 56.6–87.34 MPa [22,42,43]). Due to its excellent chemical resistance, it is a common material for tubing and connectors in HPLC and MS. Furthermore, PEEK is biocompatible and has been both used in several medical applications and as an alternative to implantable metal materials [44–47]. As PEEK is a thermoplastic, components can be fabricated by FDM, but not with conventional cost-effective printers because higher extruder temperatures of 350–450 °C and bed temperatures of ~170 °C are required [42,48]. Furthermore, an ambient temperature of ~80 °C around the printing area needs to be maintained to reduce warpage [42]. Porous PEEK parts can be made by selective laser sintering (SLS) [49,50]. Due to the limited availability of commercially available FDM printers that can provide the required high temperatures for printing PEEK, prototyping of PEEK devices for MS is usually not feasible even though PEEK has excellent properties for these applications.

2.1.5. Functionalized FDM materials

In addition to common materials, different functionalized materials for FDM printing are also available, two of which have notable properties that have been leveraged for MS applications (see Section 3). The first category is the combination of a thermoplastic doped with graphene, carbon nanotubes, or similar to render the final material conductive. This material can be used for the direct printing of electrodes, and if a dual-head printer is used, then conductive and non-conductive elements can be alternatingly implemented into a single, reproducibly assembled 3D-printed part [51–55]. Another functional class of hybrid materials is the combination of a non-water soluble thermoplastic with a water-soluble polymer, such as polyvinyl acid (PVA). By placing the printed structures into water, the water-soluble part is removed, resulting in a more flexible, somewhat porous material. These materials have been used as sorbents for SPE in both offline and online modules to improve MS analysis [56–58]. Furthermore, the flexibility of the material can be employed to create tighter seals between rigid materials.

2.2. Laser-based 3D printing

2.2.1. Stereolithography

Stereolithography (SLA) printers use photocurable resins to produce parts by solidifying the resin through photopolymerization with a UV laser. Therefore, SLA materials require photocurable moieties such as epoxy or methacrylate monomers. Material properties are tuned by the monomer composition, the concentration of crosslinkers and photoinitiators in the resin, and by the curing conditions. The composition of most commercially available resins is proprietary and are often just indicated with a product name. Commercially available SLA printers typically achieve XY resolutions of around 50 μm and Z resolutions around 10 μm. SLA-printed parts have low roughness and are therefore great for microfluidic applications where laminar flow is desired. A significant advantage of SLA printed parts compared to parts made by FDM is their liquid and air tightness. Wang et al. used SLA printing to fabricate “matrix-free” MALDI target plates by adding graphene to the photocurable resin [59]. Alternatively, Fialova et al. used FDM printing to successfully fabricate MALDI target plates. The porosity of the FDM printed target plates was disadvantageous and led to both retention of solvent in the part and to longer pumping times to remove the solvent [60]. Wang et al. chose SLA printing to construct elution chambers for gel electrophoresis devices coupled with ICP-MS because FDM-printed parts made of PLA and ABS did not

provide sufficient air-tightness [61]. Similarly, Sosnowski et al. considered using FDM to fabricate a 3D-printed liquid microjunction solvent sampling probe coupled to ESI-MS, but switched to SLA printing due to leaking connections and the clogging of fabricated channels caused by the lower resolution of FDM printing. Furthermore, they reported that the high-temperature SLA resin they chose was compatible with methanol [62]. Garcia-Montoto et al. utilized an epoxy resin to build a microflow nebulizer for ICP-MS due to its compatibility with tetrahydrofuran and its temperature stability up to 250 °C [63]. A disadvantage of laser-based 3D printing, such as SLA, is its limitation to photopolymers that are usually not biocompatible due to residual initiators and monomers [64–66].

Silica glass has exceptional properties that are desirable when chemicals are handled. It possesses outstanding chemical, mechanical and thermal resistance, high optical transparency, and is electrically insulating. However, these properties also make shaping and processing of silica glass very challenging. Kotz et al. demonstrated the fabrication of fused silica glass components by SLA printing using a photocurable silica nanocomposite [67]. If the commercial availability of SLA printing of silica glass increases, then it is a material that should be considered for MS interfaces. Accessibility to cost-effective prototyping techniques of silica glass would allow optimization and fast fabrication of parts that require high-temperature resistance such as plasma ionization probes, high-temperature reaction chambers for MS, or reaction chambers for GC-MS.

2.2.2. Polyjet

Parts made by polyjet printing are based on photocurable resins and have therefore similar properties to parts fabricated by SLA printing. In polyjet printing, the resin is deposited via nozzles onto the part and then cured by UV light for each layer. This technique enables fabrication of parts with excellent resolutions down to tens of micrometers [68,69]. However, these great advantages come with high costs for printer acquisition and resins. Polyjet printers commonly feature multiple inkjet nozzles that allow for fabrication of parts made of different materials, which is not currently possible by SLA printing and SLS where the part is built up from a bath/bed filled with a single material. Jacobs et al. used the multi-material-capability of polyjet printers to combine materials with different properties to fabricate ultrafiltration devices. A rigid material was used to maintain the structural integrity of the filtration device during ultracentrifugation and was combined with a flexible/rubber-like material to form liquid-tight seals with filter membranes that were incorporated into the device [70].

2.2.3. Selective laser sintering

Selective laser sintering (SLS) is an additive manufacturing method used to make plastic, metallic and ceramic objects. The method uses a laser to heat and bind powder particles together. Once the laser finishes solidifying the parts of the powder of one layer, a roller distributes a new layer of powder on top of the previous one. As with the resolution of SLA printing, the resolution of SLS-printed parts is mostly determined by the laser used and structural tolerances, and is therefore on the order of tens of micrometers. Due to its high acquisition costs, SLS printers are not as popular as FDM and SLA printers. An advantage of SLS printing is that it allows for fabrication of parts made of metal alloys or ceramics, which provide excellent chemical inertness and mechanical stability. Furthermore, porous materials can be fabricated by partially sintering particles and beads by controlling the laser power, speed, and temperature used. Kulomäki et al. took advantage of the porosity tunability to fabricate metal scavengers for the detection of mercury by ICP-MS [71].

3. Applications of 3D printing for mass spectrometry

The applications of 3D printing for MS have been categorized into 3 sections, according to their place in the analytical workflow. The first step for any MS experiment is the acquisition and preparation of the sample(s) to be analyzed (Section 3.1). The development of a reproducible and efficient workflow is important in quantitative chemical analysis. The first step involves the selective enrichment of low concentrations of contaminants or biomarkers from a complex sample. The compounds of interest are then introduced to the mass spectrometer as gas-phase ions. The process involves analyte desorption, ionization and transport into the vacuum of the mass spectrometer (Section 3.2) and requires ion sources and ion guides. Finally, the front end of the MS can be streamlined by combining platforms, housings or interfaces (Section 3.3) to improve sample utilization and workflow.

3.1. Sample preparation

Mass spectrometry can be hampered by sample complexity due to ion suppression/enhancement. As a result, sample pretreatment is often a crucial step for MS analysis, and can have a tremendous impact on the quality and result of the analysis. Therefore, the way in which a sample is treated can significantly influence the overall quality of the experiment. In the next two sections, the benefits, and limitations of 3D-printed modules for off- and online sample handling are discussed. Such modules can help in sample collection, storage, and preparation, for analysis with MS (as well as other types of analysis) by sample clean-up, separation, mixing with solvents, integration, or automation. Some of the examples below were not used directly in an MS-based analysis, but are included here nonetheless, as their implementation potential into such a workflow is clear [18,70,72–74].

3.1.1. Offline sample preparation

Offline sample preparation with 3D-printed devices that have been, or can be, coupled to MS detection are presented in Table 2, and mainly focus on ultrafiltration [70], SPE (Fig. 2A–B) [18,57,58,71,75], liquid-phase micro-extraction (LPME) [73,76], or creating devices for integrated, high-throughput sample pretreatment (Fig. 2C) [77–79]. In many of these applications, the 3D-printed part is a component of a larger device, or can be combined with a non-printed material, such as through the inclusion of extraction material [18,75], a stir bar [18], well plates [78], or micro-extraction tips [79]. CAD software improves part compatibility by enabling one to model the interaction of 3D-printed parts with external objects, surfaces and instruments.

Parts with functional materials can be printed, as well as external parts and structural components. This is the case in some SPE applications, where the sorbent, or stationary phase, for the extraction itself can be printed as monolithic porous structures to increase the surface area of the material to improve extraction [57,58]. Such porous materials can even be printed into a single part with a non-porous material and connected to different system components using dual-head printing [57].

These customized solutions allowed researchers to reduce the time for experiments [18,78], improve both the experimental protocols and reproducibility [58], simplify setups [57,73,75–77,79], and improve limits of detection [71]. The development of 3D-printed, offline, sample-preparation devices for an analytical workflow can be regarded as low-hanging fruit, as it does not require integration with instrumentation or compliance with the requirements of pressure, valving, solvent selection and flow rates that come with it. At the same time, as both storage and transportation can have a detrimental effect on the sample, a swift and

Table 2
3D-printed devices for offline sample preparation.

Publication (author and year)	Description	MS interface	Gains	Application(s)	Printer; material	Ion source/ MS type
Wang et al. (2016)	3D-printed 96-wellplate format for the release of N-glycans from glycoproteins, separation via dialysis, and labelling	n/a	Reduced analysis time from 3 days to 1 day.	PNGase F-mediated release of N-glycans from fetuin , followed by 2AB labeling	Not reported	MALDI-TOF
Kataoka et al. (2017)	3D-printed microfluidic chip packed with stationary phase for SPE	n/a	Inexpensive, easy-to-make SPE chips	Sample pretreatment of petroleum	FDM; PLA	GC-QqQ; FT-ICR-MS
Konieczna et al. (2018)	3D-printed sorbent that fits in a standard centrifuge tube	n/a	Minimize potential errors due to reproducible fabrication, elimination of carry-over due to disposability	Extraction of steroids from human plasma	FDM; LayFOMM 60	HPLC—ESI-Q
Kalsoom et al. (2018)	3D-printed passive sampling device with 3D-printed membrane	n/a	Fully 3D-printed sampling device, with membrane and support structure, that does not require additional parts	Atrazine in artificial seawater	FDM; PLA/PoroLay Lay-felt	GC-Q
Medina et al. (2018)	3D-printed microsystem for dispersive liquid-liquid microextraction	Operated via injection valve; offline elution	Easy preparation of complex flow systems in a variety of materials	Determination of parabens in tap water	SLA; Clear photoresin FDM; PETG	n/a
Kulomaki et al. (2019)	3D-printed porous monolithic SPE material	n/a	Preconcentration of analyte, monolithic material that requires no packing procedure	Determination of trace Hg in natural water samples	SLS; PA-12 powder with thiol-functionalized silica	ICP-QqQ
Harney et al. (2019)	3D-printed 96-plate format for sample preparation with StageTips	n/a	High-throughput sample preparation in customized platform	Proteomics analysis of human plasma during fasting	FDM; HIPS	nanoUHPLC-nanoESI-Q-Orbitrap
Huang et al. (2020)	3D-printed system with sample loading/extraction, filtration/ elution, and sample collection modules	n/a	Multi-step and high-throughput purification of small-volume complex biological samples	Analysis of multitude of toxic compounds in tap water, lavage fluid, serum and whole blood	SLA; unspecified resin	MALDI-TOF
Dominguez-Tello et al. (2020)	3D-printed holder for hollow-fibre liquid-phase microextraction	n/a	Facilitate ease-of-use of the extraction process	Determination of disinfection by-products in drinking water	FDM; PLA	GC-EI-LIT
Jacobs et al. (2020)	3D-printed centrifuge-enabled ultrafiltration device	n/a	Low-cost size-based separation	Determination of Zn^{2+} affinity for human serum albumin with different glycation levels	PolyJet; Veroclear & Tango+	n/a
Srámkova et al. (2020)	3D-printed magnetic stir cage for SPE	n/a	Integration of a stir bar into the cage with fibrous SPE material allowed for dispersion during extraction, decreasing required extraction time	Analysis of bisphenols from river water	FDM; PP, PET, PLA co-polyester with bio monomer (CPE-HG 100 extrafill), PA	HPLC; no MS

user-friendly on-site sample pretreatment protocol carried out in a 3D-printed device may aid in mitigating that risk. Moreover, as samples can be immediately submitted for the analysis, the time from sampling to answer can be decreased. Given the fact that most of the applications of these devices fall into medical research [58,70,77–79], or environmental safety [18,57,71,73,76], where sample is gathered outside the lab and thus normally needs to be collected, stored and brought to the laboratory, such an offline approach is perfectly justified. While some of the reported devices have been demonstrated in an offline mode, they could be used in an online fashion as well (e.g. flow-through SPE systems that could be connected directly via a valve to an (HPLC-)MS (see also Section 3.1.2)) [73,75].

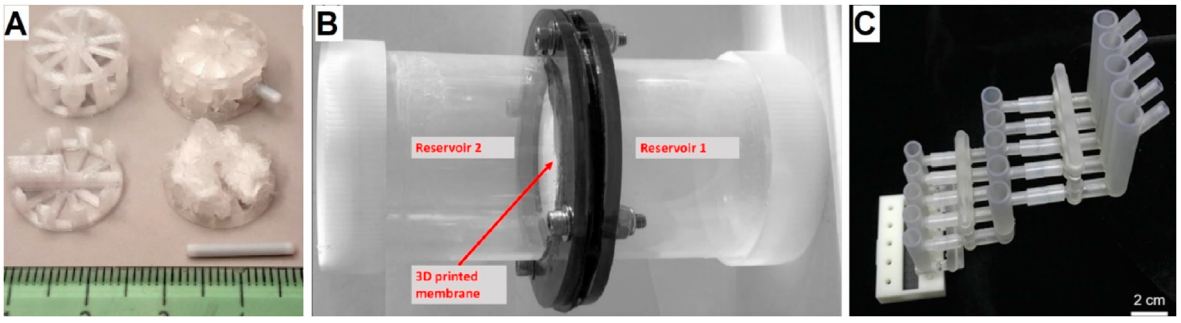

Fig. 2. Examples of 3D-printed, offline, sample-preparation modules. (A) Fiber-based dispersive SPE for the extraction of bisphenols; Adapted with permission from Sramkova et al. [18]. Copyright 2020 American Chemical Society. (B) Flow-through absorption through a 3D-printed sorbent for the extraction of atrazine from artificial seawater; Adapted with permission from Kalsoom et al. [57]. Copyright 2018 American Chemical Society. (C) Modular sample-preparation setup for increased throughput analysis of toxic compounds from tap water and biological samples. Reproduced from Huang et al. [77] with permission from The Royal Society of Chemistry.

Table 3
3D-printed devices for Online Sample Preparation.

Publication (author and year)	Description	MS interface	Gains	Application(s)	Printer; material	Ion source/ MS type
Mathieson et al. (2013)	3D-printed configurable reactor with real-time MS analysis	Coupled to ESI source	Easily change reaction stoichiometry, real-time continuous MS analysis of products	Supramolecular chemistry	FDM; PP	ESI-Q-TOF
Frizzarin et al. (2016)	3D-printed holder to position magnet over a microchannel to trap magnetic SPE particles	Coupled via injection valve	Alignment of magnets with flow system	Determination of anionic surfactants in natural water samples	Not specified	n/a
Scotti et al. (2017)	3D-printed reactor cartridge with internalized stir bar and integrated nanoESI emitter	Cartridge in 3D-printed device for fluidic connections, magnetic stirring, and positioning	Passive and direct sampling from reaction mixture, integrated agitation of reaction mixture	Characterisation of a Diels–Alder reaction and the subsequent retro Diels–Alder reaction	FDM; PP	nanoESI-3D IT
Jönsson et al. (2017)	3D-printed holder for connecting an enzyme-digestion chip directly to LC-MS	3D-printed holder is used to couple a microfluidic element to LC-MS	Allows use of pressures up to ~46 bar; online coupling of microfluidic device to LC-MS system	Pepsin digestion of haemoglobin	FDM; PLA	nanoUHPLC-ESI-Q-TOF
Wang et al. (2017)	3D-printed microflow injection valve and 3D-printed magnetic SPE holder	Coupled via injection valve	Customized, multifunctional injection valve, scaffold for online SPE	Trace analysis of parabens and triclosan in urine and saliva	SLA; Formlabs Clear Resin	HPLC; no MS
Scotti et al. (2019)	3D-printed stainless steel microreactors with ESI emitter	Positioning in a 3D-printed holder for fluidic connectors	Sample preparation, mixing, and spray generation from a single, stainless steel device	Inverse electron demand Diels-Alder and subsequent retro Diels-Alder reaction	SLS; 316L stainless steel powder (median particle size of 31 μm)	ESI-3D IT
Su et al. (2019)	3D-printed porous (interlaced cuboids) SPE material and cartridge	Coupled via injection valve	Monolithic SPE column that requires no packing	Speciation of iron in surface water	SLA; acrylate resin	ICP-Q
Häbe et al. (2020)	3D-printed platform for zone elution in planar chromatography	3D-printed, interface for elution-head-based TLC/HPTLC-MS	Efficient and user-independent TLC/HPTLC-MS automation	Analysis of azofloxine and butyl paraben	FDM; PLA	ESI-Q-Orbitrap
Tascon et al. (2019)	3D-printed holder containing an embedded rare-earth magnet for a particle collection step	LMJSSP couples sample plate to ESI	3D-printed holder can be directly coupled to ESI via LMJSSP	Prohibited substances in PBS and human urine using Fe_2O_3 magnetic nanoparticles (50 nm) functionalized with C18	FDM; nylon	ESI-Q-TOF
Sosnowski et al. (2020)	3D-printed LMJSSP coupled to ESI-MS	Connected to ESI-source; operated manually or via robotic auto sampler	3D-printed sampling unit coupled directly to MS; analysis in less than 1 min and without any sample preparation	Detection of pesticides on fruit peel surfaces and illegal substances in home-made pills, q uantification of DoA in urine and plasma	SLA; High Temp. Resin	ESI-QqQ
Su et al. (2020)	3D-printed SPE cartridge	Coupled via injection valve	No column packing required; operated by low-pressure peristaltic pumps; Low background signal; extraction efficiency >99.2%	Enhanced extraction of multiple metal ions	FDM; ABS, Lay-Fomm 40, Lay-Fomm 60, Gel-Lay, and Lay-Felt	ICP-Q

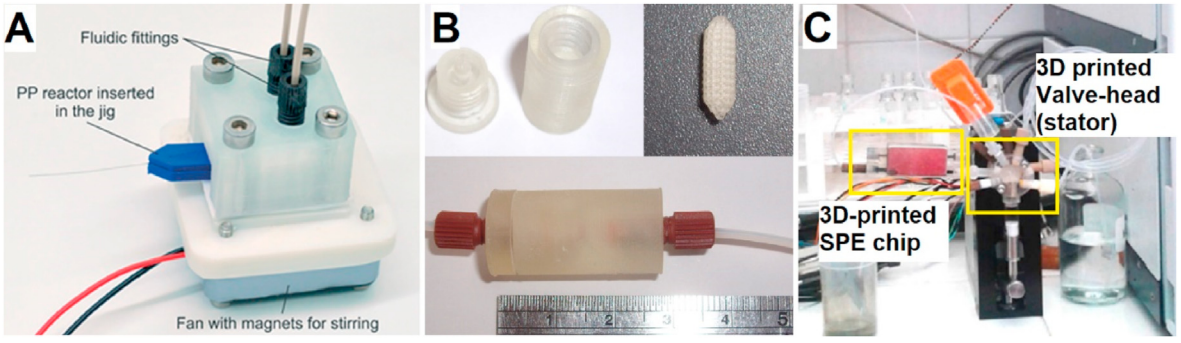

Fig. 3. Examples of 3D-printed online sample preparation modules. (A) A flow chemistry cell with integrated stir bar and emitter, in a 3D-printed platform for positioning; reproduced from Scotti et al. [39]. Published by The Royal Society of Chemistry. (B) 3D-printed sorbent and column for online SPE of iron in surface water; reproduced from Su et al. [82] with permission from Elsevier. (C) 3D-printed valve stator and magnetic-bead-based SPE for analysis of parabens and triclosan; adapted with permission from Wang et al. [72]. Copyright 2017 American Chemical Society.

3.1.2. Online sample preparation

Online sample handling or treatment is more restricted than the offline variant, due to the need for system compatibility. Still, numerous examples of online coupling of devices to an MS have been reported since 2013; these can be divided into online flow chemistry and online extraction (summarized in Table 3).

The first example of online flow chemistry is the dynamic/real-time adjustment to the stoichiometry of a chemical reaction in a 3D-printed PP reactor, the products of which could be directly monitored with MS [41]. After this initial report, other flow reaction systems have been demonstrated, such as one fully printed in stainless steel, with an integrated electrospray emitter [80]. While this is on the higher end of the price spectrum, 3D-printing in metal can allow fabrication of a fully integrated MS microreactor/emitter with one press of the button [80]. Another 3D-printed reactor printed with PP incorporated additional functional elements including a magnetic stir bar and a separate emitter (Fig. 3A) [39]. FDM 3D printing was used in this example, as it enabled one to stop during a print to insert an additional material, such as a stir bar, allowing the highest level of flexibility while printing.

The integration of external components, or parts made from different materials has also been demonstrated in most online extractions using 3D printing. For example, online sample extraction was achieved with magnets integrated into 3D-printed parts that were used in combination with paramagnetic particles with functionalized surfaces [72,74,81]. This integration of non-3D-printed objects by integration/enclosure of solid objects for sample preparation steps is beneficial for a fully integrated approach. Interestingly, it is possible to obtain FDM printable materials with additional functionality, such as conductive or magnetic properties. The use of such materials could make further developments even more straightforward, for example by directly printing magnetic or conductive elements into the device as well. However, this would require further improvement in terms of dual-head/multi-material printing, which is often problematic due to clogging issues. Moreover, polymers that are doped with particles are more difficult to print and can lead to an increase in clogging frequency or damage to the extrusion nozzle. Besides using magnetic particle-based extraction for facilitating online sample extraction [72,74,81], interlaced [82] or porous [56] 3D-printed monolithic sorbents for SPE have also been used (Fig. 3B). In all cases, valves were needed to decouple the extraction phase from the elution and analysis phase. If needed, components of a flow injection system, like the stator of the valve, can be modified through CAD software, 3D printed, and then applied in the setup to enhance system integration (Fig. 3C) [72].

Finally, 3D printing has been described for the realization of online sampling systems which allow the direct or real-time analysis of surfaces. For example, 3D-printed systems have been demonstrated for the online, solvent-based sampling of surfaces with a liquid micro-junction surface-sampling probe (LMJSSP) [62,81]. Moreover, 3D-printed modules for connecting and supporting subsequent setup modules have also been published, such as the connection between a microfluidic enzymatic chip and a UHPLC-MS system [20], as well as an entire platform to couple thin-layer chromatographic separation to MS analysis of the individual bands by elution-head-based extraction [83].

Current limitations of 3D-printed online modules for MS stem from the fact that the plastic devices can only tolerate limited amounts of pressure before they delaminate and start to leak, which is in part due to their layer-by-layer fabrication process. Moreover, most of these materials have limited solvent compatibility (see Section 2). Finally, due to the limited resolution of 3D-printed devices, it might be more appealing to use microfluidic systems produced via conventional microfabrication, such as soft lithography, which generally has better resolution [84]. However, those fabrication processes are more costly, much more complex, and therefore require adequate training to execute.

3.2. Ion introduction

Mass spectrometry is a family of instrumental techniques that uses different technologies including quadrupole, ion trap, time-of-flight, sector instruments, FT-ICR and Orbitrap to make low and high resolution mass measurements. One thing all instruments have in common is that they separate gas-phase ions based on their mass-to-charge ratios. Both the generation of gas-phase ions and their introduction into the vacuum at the front end of the MS impacts the method sensitivity. This 'front-end' of the MS, including ion sources and ion guides, is generally more accessible to the researcher than the interior of the mass analyzer, and has been a subject of constant change and innovation. Consequently, 3D printing has been used to fabricate a number of interesting designs and configurations, producing innovations that have enabled it to gain a foothold in this scientific area.

3.2.1. Ionization

Ambient ionization mass spectrometry (AIMS) is a rapidly expanding family of techniques for straightforward analysis of samples under ambient conditions [85]. AIMS can also be viewed as a collection of highly creative solutions to specific problems with respect to the introduction of a wide variety of sample types to an MS. While some AIMS approaches have experienced a broader acceptance and implementation, such as DESI [86] and DART [87], most AIMS sources remain prototypical instruments with only a few existing copies world-wide. This hampers the potential for such innovative solutions to be used in other labs, where there may be a direct need for such a specific solution. As a result, those approaches that are the most straightforward in their minimalistic embodiment have found broad applicability in the scientific community. A key example of the latter is paper spray (PS) ionization [88], in which electrospray is generated from a paper tip by application of solvent and a high electrical potential. Paper spray essentially requires only a conductive clip, a triangular piece of paper, a high-voltage supply, and some solvent. However, to make PS-MS truly user-friendly, and applicable to routine analytical chemistry practise, a more modular approach is warranted. For this reason, both in commercial and in research instrument settings, cartridges have been developed for PS-MS to achieve a more user-friendly, robust and reproducible user interface.

While the first such cartridge was demonstrated by injection molding [89], shortly after, the first 3D-printed cartridge was reported [19]. Ultra-fast prototyping made 3D printing attractive for this development. The first 3D-printed PS cartridge (Fig. 4A) was the result of iteratively designing, printing, characterizing, and evaluating over a 100 different versions of the device to optimize its structure [19]. The obtained structure contained 3D embedded channels, reservoirs, electronic connections, and a slide-and-click lid with solvent-guiding structures. CAD and 3D printing allowed the fabrication of a highly complex but inexpensive disposable cartridge. Not only did this cartridge provide protection, improved accuracy of positioning, and stability for the paper tip, but it also implemented sophisticated solvent control to allow fast wetting of the paper tip and prolonged solvent supply for continuous spray. This cartridge was later improved upon (Fig. 4B) by the embedding of a metal focusing lens, which was inserted during the printing of a single part [90]. In that same part, a manifold of open tubes was integrated to allow the distribution and release of desolvation gas around the spray tip. Another cartridge for controlled solvent delivery to the tip was published [34], which embodied a more direct

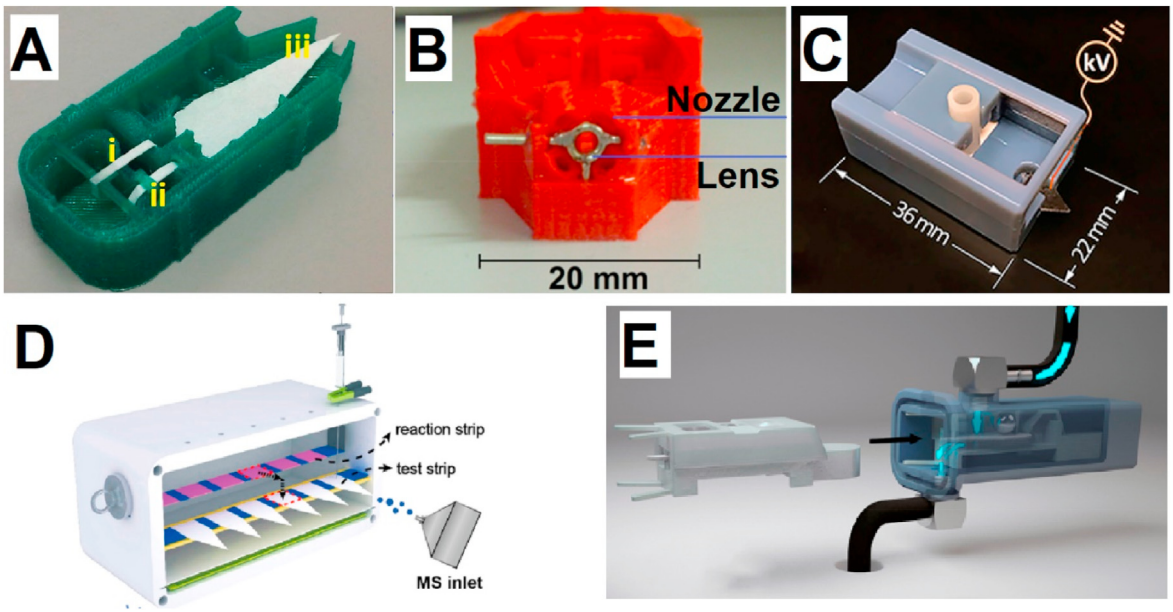

Fig. 4. Overview of 3D-printed cartridges for paper spray ionization that add functionality. (A) Cartridge with integrated solvent control, including (i) a solvent reservoir, (ii) wicks for solvent delivery to (iii) the paper tip; adapted with permission from Salentijn et al. [19]. Copyright 2014 American Chemical Society. (B) Cartridge for ion focusing and desolvation; adapted with permission from Salentijn et al. [90]. Copyright 2017 American Chemical Society. (C) Cartridge with cylindrical SPE column; adapted with permission from Zhang et al. [92]. Copyright 2017 American Chemical Society. (D) Cartridge that combines an enzyme reactor to PS-MS; adapted with permission from Yang et al. [93]. Copyright 2019 American Chemical Society. (E) 3D-printed cartridge holder for on-paper collection of aerosol sample; adapted with permission from Dhummakupt et al. [94]. Copyright 2017 American Chemical Society.

solvent supply system through the integration of a channel structure in the 3D-printed part. Both systems extend spray times well beyond non-cartridge-based PS, which is beneficial for improving signal and allowing on-paper separation.

While some later work on cartridges for PS mostly revolved around improving the ease and accuracy of positioning [91], other work truly aimed to further increase device functionality allowing more complex analytical operations with PS by the incorporation of sample-handling modules. In one such development, the integration of an on-cartridge SPE module was demonstrated, in which immunochemical enrichment of proteins could be performed by loading the SPE column with sample that then was absorbed in a sink pad (Fig. 4C) [92]. By switching the position of the column above the paper tip, and eluting the analytes, these could be directly analyzed with PS-MS. In a second system, a 3D-printed sample treatment module was used to perform an enzymatic reaction on a paper based substrate (Fig. 4D), that could afterwards be easily moved onto the paper spray tips, which were then used for the analysis after passive sample transfer [93]. A third approach describes a 3D-printed device that could be connected to a commercial (non-3D-printed) cartridge for the direct capture of chemical warfare agents in aerosol onto the paper substrate in the cartridge (Fig. 4E) [94]. These examples of 'click-and-collect' or 'sample-and-slide' devices can incorporate additional sample handling steps. The use of 3D printing allows easy customization of such devices for different applications.

While PS-MS has led to the most diverse innovative 3D-printed solutions, other AIMS techniques have also benefited from additive manufacturing. For example, the designs for a largely 3D-printable Low Temperature Plasma (LTP) probe have been published [11], which have since been applied to the classification of tequila and mezcal products [95], as well as analysing active compounds in plants, such as mescaline in cactus and nicotine in tobacco seedlings [96]. In the original paper, the design and *stl files were made publicly available so that other researchers can easily build or modify such a tool in house. This again highlights crucial benefit of additive manufacturing, through which the spreading of scientific expertise in instrumentation is greatly facilitated. This development is a good example of the current drive towards open-access science, and the increased availability of 3D printing. In other work, a simplified, 3D-printed holder for a dual-electrode glow discharge source was demonstrated [97]. For ICP-MS, a 3D-printed total consumption microflow nebulizer was reported, where tubing was integrated into the printed part [63]. These are good examples of how 3D printing assists in the rapid prototyping of a device where functional elements (e.g. electrodes or tubing) are assembled and aligned. Similarly, a rotary holder for nanoESI emitters was published that allows the monitoring of different reactions running in parallel, by continuously changing the spray tip in front of the MS [98]. In addition to the incorporation of non-printed elements, this shows how easily 3D printing allows the customization of the setup to increase its functionality in a straightforward and user-friendly manner.

Finally, for DESI, 3D printing could improve performance by printing sample plates with wells from which the desorption process was reported to be more efficient, leading to improved sensitivity [15], or even printing an entire DESI setup that could be connected directly to the MS [99]. There are some other examples of surface-based desorption/ionization, such as using an SLA-printed, graphene-doped polymer for allowing MALDI, without the need of matrix [59]. The latter is a good example of using functionalized 3D printed materials to improve mainly the operational simplicity of a method. This approach was later also demonstrated with FDM printing, though the resulting plates were not tested without matrix [60]. While currently not yet demonstrated, combining enhanced surface analysis with integrated device functionality would be a powerful tool towards simplified analysis of very complex samples. Table 4 summarizes all the 3D-printed ionization sources described here.

Table 4
3D-printed devices for ionization.

Publication (author and year)	Description	MS interface	Gains	Application(s)	Printer; material	Ion source/MS type
Salentijn et al. (2014)	3D-printed cartridge with controlled solvent supply for PS-MS	3D-printed holder on 3D translational stage	Slow and fast wetting system, prolonged spray duration up to 50 min, positioning of the paper tip, protection	Separation of dyes, analysis of lidocaine	FDM; PLA	PS-Q
Duarte et al. (2016)	Cartridge for a paper tip to improve spray stability, with microfluidic channel to extend spray duration	3D-printed platform for positioning in front of MS	Extended spray duration up to 10 min, improved stability and ease of positioning	Blue and red pen inks, methanolic solutions of caffeine, xylose and lysozyme	FDM; ABS	PS-LIT
Elviri et al. (2016)	3D-printed surfaces for sample deposition and DESI-MS	Printed plates placed on ion source platform	3D-printed plate geometries improved the analytical sensitivity	Standard solutions of insulin and gentamycin	FDM; PLA	DESI-LIT-Orbitrap
Martínez-Jarquín et al. (2016)	DIY low-temperature plasma ionization device	Positioned with a clamp on a stand in front of MS	Reproducible analysis of solid, liquid and gaseous samples with spatial resolution of 200 μm	Surface Analysis of vanillin standard, camphor tablet, aspirin, norecil, clove of garlic, and cinnamon bark	FDM; ABS, PLA, PC	ESI-3D IT
Salentijn et al. (2017)	3D-printed PS cartridge with integrated tubes for desolvation gas and an electrostatic lens	Cartridge is positioned in 3D-printed holder that can be attached to the MS	Improved spray stability; increased desolvation	Standard solutions of lidocaine and prilocaine	FDM; PLA	PS-Q
Dhummakupt et al. (2017)	3D-printed device for aerosol capture onto commercial PS cartridges	Connects to commercial PS cartridges, which are placed in a commercial PS source	Direct sampling of aerosol on a PS substrate; no extraction required	Sampling and analysis of chemical warfare agents	SLS; glass-filled nylon materials Polyjet; Veroclear	PS-LIT – Orbitrap
Martínez-Jarquín et al. (2017)	3D-printed LTP probe	Placed in front of MS, samples moved to the probe via a robot	In comparison to a DIESI system, the LTP was faster and required no pumps	Classification of Tequila and Mezcal products	FDM; material not specified	LTP-3D IT
Pulliam et al. (2017)	3D-printed rotary continuous flow nanoESI holder	Positioned in front of MS	Switching between reaction vessels, up to 6 reactions over the course of hours without cross-contamination	Hydrazone formation and Katritzky transamination	FDM; PLA	nanoESI-LIT
Zhang et al. (2017)	3D-printed PS cartridge with integrated antibody enrichment column	Cartridge placed in front of MS	Preconcentration of protein target, directly coupled to PS-MS	Detection of plasma proteins, including post-translational modifica-tions	PolyJet; Veroblue	PS-Q-Orbitrap
Bills et al. (2018)	3D-printed cartridges for PS	Positioning of cartridge in front of MS	Reproducible positioning of tips of various thickness	Prescription drugs, fentanyl and synthetic cannabinoids	PolyJet; VeroBlue FDM; PLA, PP	PS-Q-Orbitrap
Wang et al. (2018)	3D-printed plates for matrix-free laser desorption ionization	Printed (MA)LDI plate	Due to doped graphene, no matrix is required for the LDI process	Low-mass environmental pollutants, synthetic polypetide	SLA; Formlabs clear doped with 0.01–0.2% (w/w) graphene	MALDI-TOF
Yang et al. (2019)	3D-printed enzyme reactor-PS cartridge	Mounted on 3D-translational stage	Easy operation, integrated enzyme reactor, multiple paper tips in cartridge	Detection of butynylcholinesterase activity	Not reported	PS-3D IT
Moreno-Pedraza et al. (2019)	3D-printed LTP	Positioned in front of MS; samples moved on controllable stage	Imaging MS with pixel size down to 50 × 50 μm^2	Mapping mescaline in a San Pedro cactus, tropane alkaloids in jimsonweed fruits and seeds, nicotine in tobacco seedlings	FDM; material not specified	LTP-3D IT
Garcia-Montoto et al. (2020)	3D-printed total consumption micronebuliser for ICP-MS	Placed in front of MS	Low-cost nebulizer, embedding PEEK tubing for organic solvent flow	Trace element analysis in crude oil	SLA; EPOXY-HT	ICP-MS (double focusing sector field)
Hoegg et al. (2020)	3D-printed frame for the assembly of a LSAP-GD probe	Placed in front of MS	Assembly of sources of various geometries for quick testing	Caffeine and triethyl phosphate	FDM; PLA	LSAP-GD-Q
Fialova et al. (2020)	3D-printed plates for laser desorption ionization	Printed MALDI plate	Inexpensive alternative for commercial target plates	Tryptic digest of BSA, BSA solution, extracts from bacteria cultures	FDM; ABS with carbon particles	MALDI; TOF
Zemaitis et al. (2020)	3D-printed DESI setup	Added onto nanospray adapter that can be directly attached to the MS	Inexpensive, easily adjustable alternative for commercial DESI source	Lipid fingerprint analysis in rat brain tissue	FDM; PLA	DESI-FT-ICR

3.2.2. Ion guides

Mass spectrometry involves the manipulation of ions through forces introduced by magnetic and electrostatic fields, which not only requires the formation of gas-phase ions during ionization (Section 3.2.1), but also the transport of ions at atmospheric pressure into the vacuum regions of the instrument. This is another important field where 3D printing has been applied in recent years, and these efforts are summarized in Table 5. It is well known that with standard ion sources (e.g. ESI, and AIMS methods, such as PS-MS) where ions have to transition from ambient air to the high vacuum in the MS, many ions are lost due to expansion of the ion beam and thus are not detected. Ion funnels have been applied to

Table 5
3D-printed ion guides.

Publication (author and year)	Description	MS interface	Gains	Application(s)	Printer; material	Ion source/MS type
Tridas et al. (2015)	3D-printed holder for a flexible circuit board as ion funnel	ESI emitter positioned in front of funnel	Comparable transmission as conventional funnel, at greatly reduced cost and simplified construction	n/a	FDM; ABS	ESI; no MS
Hollerback et al. (2017)	Fully 3D-printed drift tube for IMS	Position of emitter optimized during experiments	Resolving power as stand-alone up to 50 and 42 in positive and negative mode, respectively, operation in open air, fully 3D-printed including electrodes	Separation of tetraalkylammonium cations; drugs; sodium alkyl sulfate anions	FDM; PLA and conductive PETG containing multiwalled carbon nanotubes	nanoESI-IMS
Hollerbach et al. (2018)	Dual-gated 3D-printed IMS	Drift tube positioned in front of MS; position of emitter optimized during experiments	Operates in the open air; resolving power up to 45; can be coupled to any mass spectrometer; possesses 2 ion gates at opposite ends	Separation of tetraalkylammonium cations; amphetamines; opioids; bradykinin and angiotensin II	FDM; PLA and PETG containing multiwalled carbon nanotubes	nanoESI-LIT or nanoESI-QqQ
Draper et al. (2018)	3D-printed holder for a flexible circuit board as ion funnel-ion carpet	ESI emitter positioned in front of device	Transmits a broad range of molecular masses	HBV capsid; P22 procapsid; 0.05-μm amino-functionalized polystyrene beads (m/z > 100,000 Da); 0.1-μm amino-functionalized polystyrene beads (m/z > 200,000 Da)	FDM; ABS	ESI-Charge Detection MS
Iyer et al. (2019)	3D-printed focusing devices	Positioned at different distances in front of the MS, nanoESI emitter inserted through holes in the side	Improved transmission of ions from source to MS in ambient conditions	Standard solutions of tetraalkylammonium bromide salts	FDM; PLA, PETG containing multiwalled carbon nanotubes	nanoESI-QqQ
Hauck et al. (2020)	3D-printed unibody drift tubes with conductive and non-conductive elements	Mounted onto front of MS	Printing and assembly occurs in a single process, leading to reproducible drift tubes with improved accuracy (±0.1%) of IMS system	Characterized with 2,6-di-*tert*-butylpyridine	Dual-head FDM; PETG doped with carbon nanotubes; PETG	Corona ionization-TOF
Schrader et al. (2020)	3D-printed drift tube for FT-IMS to allow coupling to slow mass analyzers	Drift tube placed in front of MS, nanoESI emitter is placed in front of drift tube	Operated under atmospheric pressure, easy implementation	Solutions of tetraalkylammonium salts, explosives, fentanyls, and amphetamines	FDM; PLA/PHA; PETG containing multiwalled carbon nanotubes	nanoESI-LIT
Schrader et al. (2020)	3D-printed drift tubes for IMS of different lengths and curvature	nanoESI emitters placed in front of drift tubes	Rapid prototyping of drift tubes to study the optimal geometry, following simulations	Standard solutions of tetraalkylammonium salts	FDM; PLA/PHA & PLA doped with carbon black	No MS detection

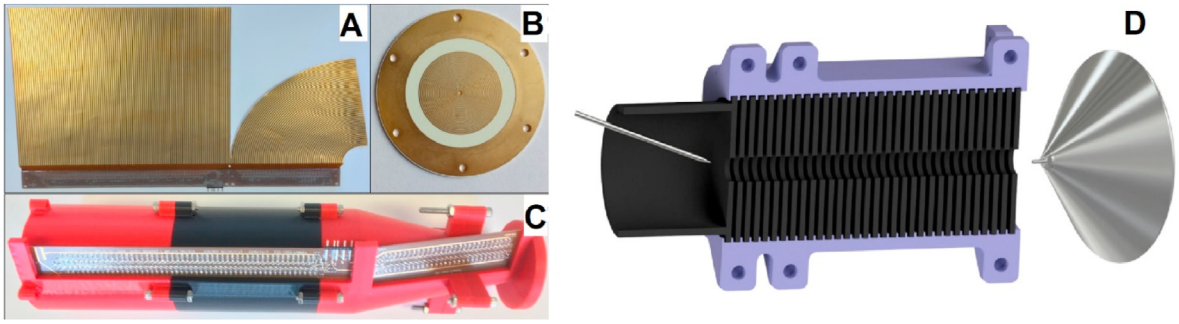

Fig. 5. Examples of 3D-printed devices for ion transport. (A–C) 3D-printed holder for a circuit board to shape it into an ion funnel; adapted with permission from Draper et al. [100]. Copyright 2018 American Chemical Society. (D) Design for a 3D-printed drift tube, where black indicates conductive and blue nonconductive printed parts; adapted with permission from Hollerbach [53]. Copyright 2018 American Chemical Society. (For interpretation of the references to colour in this figure legend, the reader is referred to the Web version of this article.)

focus ions during this transition, yet these are typically complex and costly devices. Recent work has focused on employing a 3D-printed frame to configure a one-piece, printed-circuit board into an appropriate shape to allow ion manipulation/focusing (Fig. 5A–C). The ion funnel produced has been proven to be as efficient as a conventional funnel, but lighter, easier to fabricate and less expensive, with lower power consumption [36,100]. These properties contribute to making truly portable MS systems feasible.

A different type of ion guide, the drift tube used in ion mobility spectrometry (IMS), can similarly be 3D printed (Fig. 5D) [52,53,101]. Where in the previous example, only the funnel housing was 3D printed, here, the authors used a carbon nanotube-doped polymer for FDM printing of the electronic parts, as well as the non-conductive elements of the ion guides. The drift tube could be used in different setups, namely for stand-alone IMS, as well as hyphenated to an MS instrument [52]. Initially it was reported that the drift tube could only be used by instruments with a fast mass analyzer (such as TOF), but coupling to a slower analyzer (such as an ion trap or Orbitrap) has also been demonstrated through the implantation of a dual-gated system [53], or by Fourier Transform IMS [101].

One of the most attractive features of using 3D printing for the development of ion guiding structures is the very short time

between running simulations to estimate ion trajectories, and the experimental verification of those simulations. Due to its low cost, ease of fabrication, and short production time, many different designs can be rapidly tested, as was done for 3D-printed focusing electrodes [54], and for 3D-printed drift tubes with one or multiple turns [55]. Importantly, the use of CAD software allows the precise definition of dimensions of a device – and these are then simply passed on to the printer for production, resulting in appropriate alignment between, in this case, conducting and insulating ring elements in a drift tube or ion funnel. Moreover, it has been demonstrated that the use of dual-head FDM printing, which allows the printing of multiple materials in a single part, can improve upon this further by combining production and assembly processes, leading to a unibody drift tube and thereby increasing the reproducibility of device fabrication. Obviously, as is well-known, additive manufacturing via FDM is characterized by some variability in the thickness of printed features [84], usually in the range of several hundred micrometers. However, the alignment and macrostructure reproducibility is excellent [51].

3.3. Platforms

Any work published thus-far on the application of 3D printing for MS analysis has been on the front end of the MS, and includes sample handling, improved ionization, and ion transmission. However, as such systems are developed, their implementation into a robust setup or workflow is as important as the scientific innovation in the parts themselves. Before 3D printing, the positioning of novel ion sources in front of an MS would be achieved by clamping them to a support; hyphenation of instruments would occur via tubing in open air, or samples would be transported in an offline fashion from one setup to the next. However, 3D printing is also being increasingly applied to solve such interfacing and system integration challenges.

3.3.1. MS interfaces

At the core of an MS interface is the ion source (Section 3.2.1), but connecting or positioning a source to the inlet of the MS requires additional components. Typically, commercial ESI sources utilize a metal-and-glass bulb around a small spray needle, that can be mounted to the front end of the MS and contains all connections for solutions, gases and high voltage. This is also the interface that is used for many of the sample-preparation applications of 3D printing (Section 3.1), where for example SPE is performed, and the purified extract is injected in an offline or online manner. In both online and offline sample preparation, the (ESI) interface with the MS can remain unaltered, but requires an interface/connection at an earlier stage which can be realized using a flow injection valve [56,72,82] or direct in-line coupling [41,80].

In the case of novel ion sources, cartridges for AIMS methods, or ion transmission devices such as the funnel or drift tube, the above is clearly not applicable. In many cases, the chosen solution is based on the placement of the device in front of the source-less MS without attaching it to the instrument. This is the approach most often followed in ambient methods, including paper spray [19,34], LTP ionization [11], and IMS [53]. This brings certain advantages: (i) the ease with which such methods can be coupled to different instrument types, since there are no universal connecting mechanisms for different source-instrument combinations; (ii) possibility for positional optimization to improve ion transmission; (iii) more flexibility when altering the device dimensions. Despite not being directly attached to an MS, 3D-printed platforms can still assist in the positioning of devices, such as a cartridge. At the same time, such unconnected interfaces suffer from (i) reduced positional reproducibility, (ii) the necessity for more bulky setups in front of the instrument, and (iii) generally a more open interface, which is susceptible to (changes in) ambient conditions, particularly turbulent air flow. An interesting approach in this category has been to employ a 3D-printed rotary holder for nanoESI, which is a good example of how the customizability of 3D-printed interfaces greatly improves the flexibility and system integration of an otherwise complex experimental setup [102].

Additive manufacturing offers the possibility to easily build customized interfaces between source and instrument that can be attached to the instrument and overcome (some of) the aforementioned limitations. An example of this approach involves a custom holder that is mounted to an MS using the fitting as the original equipment manufacturer source (see Fig. 6A–B) [35,90], or by modifying the MS attachment with 3D-printed elements [99]. One obvious drawback of this approach, depending on printer and material selection, is that the front-end of an MS is often heated to improve desolvation. When directly attaching a customized polymer platform to this front end, it may restrict the temperature range that can be applied. An additional limitation here is the fact that such a platform would be exclusively tailored for a specific instrument or vendor. The variety in the front-end designs of MS instruments from different manufacturers remains a challenge in this regard. However, it is foreseeable that an open-access database can be developed, in which 'click-on' frameworks for different instruments are available. These could be downloaded and then further modified via CAD software to allow customization for a specific application.

A third approach to the interfacing problem is to design and produce 3D-printed parts that can be directly connected via an existing commercial interface. Examples of this approach include the use of a commercial paper spray source [94], and 3D-printed

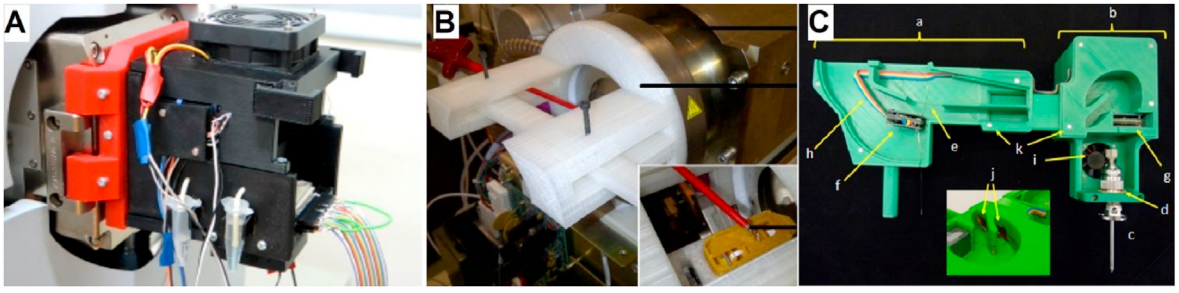

Fig. 6. Examples of 3D-printed platforms for functional elements that also serve as an interface to the MS. (A) Platform for coupling digital microfluidics directly to MS; reproduced from Hu et al. [35]. Published by The Royal Society of Chemistry. (B) Positioning a PS cartridge reproducibly in front of the MS; adapted with permission from Salentijn et al. [90]. Copyright 2017 American Chemical Society. (C) Interface between CE and MS instruments, that also integrated capacitively coupled contactless conductivity detection; reproduced from Francisco et al. [103] with permission from Elsevier.

Table 6
3D-printed housing and integration.

Publication (author and year)	Description	MS interface	Gains	Application(s)	Printer; material	Ion source/MS type
Hu et al. (2015)	3D-printed chassis for aligning digital microfluidic chips with MS	Chassis can be directly attached to MS	Direct and compact coupling of digital microfluidics to MS	Monitoring the reaction between glutathione and hydrogen peroxide	FDM; ABS	V EASI-LIT
Dutkiewicz et al. (2015)	3D-printed humidity chamber for nanoDESI	DESI stage inside the humidity chamber	Preventing evaporation of sample to improve reproducibility	Spatiotemporal profiling of topical drugs on skin with micro-patch arrayed pads	FDM; ABS	nanoDESI-LIT
Liu et al. (2015)	3D-printed platform for autosampling from digital microfluidics	Adapted autosampler	Direct sampling from the surface	Analysis of product for reaction of testosterone and quaternary aminooxy reagent	FDM; material not specified	nanoLC-ESI-QqQ
Francisco et al. (2016)	3D-printed interface for dual detection after CE separation with C^4D and ESI-MS	3D-printed interface integrates different elements of setup	Reproducible and adaptable positioning of C^4D as add-on to ESI-MS after CE	Separation of sugars at high pH, biogenic amines at low pH, carboxylic acids at neutral pH	FDM; ABS	CE-ESI-QqQ
Tycova et al. (2016)	DIY 3D-printed device for production of nanoESI emitters	n/a	Nanospray tips can be manufactured with controllable tip angle	n/a	FDM; PLA	n/a
Francisco et al. (2018)	3D-printed holder with integrated temperature control to couple CE, MS and C^4D	3D-printed integrative platform	Temperature control to combat joule heating in the CE capillary	Separation of nicotinate and monoethyl carbonate	FDM; ABS	CE-ESI; QqQ
Jönsson et al. (2018)	3D-printed holder for microfluidic chip with ESI emitter	3D-printed clamp for holding a custom microfluidic/ESI chip	Positioning of custom device in front of MS	Progesterone	FDA; PLA	ESI-LIT
Wang et al. (2019)	3D-printed systems for embedding gel electrophoresis and interfacing with MS	3D-printed system that connects to the source	Online coupling; easy optimization of hardware	Metalloproteins	FDM, PLA; ABS SLA; unspecified resin	ICP-MS (QqQ)

sample plates that fit into a commercial DESI stage [15] or MALDI source [59]. Another interesting approach has been the development of a 3D-printed manifold that allows the use of an autosampler to acquire microliter volumes of sample from digital microfluidic chips [104]. These approaches highlight one of the important advantages of 3D printing, namely that it allows the production of add-on modules to existing hardware, to seamlessly connect and integrate analytical instrumentation.

3.3.2. Housing and integration

3D printing can also be used to integrate and house the different parts of an experimental or prototypical setup; an overview is given in Table 6. Such use of 3D printing does not generally add new functionality, but nonetheless helps to reproducibly and conveniently assemble components and conduct experiments [83,104,105]. An early example of an integrative housing describes a method to connect digital microfluidics to MS (Fig. 6A), including heating, droplet collection, ionization and electronics [35]. In other work, different housings were developed to connect a capillary electrophoresis setup to an MS, to allow better control of the temperature of the capillary for improved robustness, which also integrated a capacitively coupled contactless conductivity detector (C^4D; Fig. 6C) [37,103]. Similarly, a 3D-printed box was created to house a DESI stage, which included an inlet for water vapor, to reduce evaporation of sample from the DESI plate [106]. Housing and elements of a gel electrophoresis system that could be coupled to MS were developed as well, using FDM printing for larger parts, such as the housing, and SLA for parts that required higher reproducibility/precision, such as a gel tube [61]. Tycova et al. developed a tool for production of nanospray emitters for capillary electrophoresis, and the designs were made openly accessible [107]. These are all examples of how CAD in combination with 3D printing can be used to develop organized analytical systems that help to streamline research and increase the availability of otherwise difficult-to-obtain or expensive materials or tools. Moreover, if parts need replacement, or adaptation due to new insights, the part can be easily redesigned and the long design, make and test cycle associated with a traditional machine shop mitigated.

4. Conclusion and future directions

It is important to notice that the number of papers per year on 3D printing for enhancing MS is still increasing. This trend will likely continue as there is additional interest from the scientific community to leverage this technology and more and more labs are becoming outfitted with 3D printing infrastructure. The examples presented here, which demonstrate the developments in this area from 2013 to 2020, show numerous exciting directions, which are briefly addressed below.

Customization and Integration: The most straightforward use of 3D printing lies in its unprecedented capacity to customize lab setups, design auxiliary elements or enable system integration. This is incredibly valuable to create more robust and reproducible experimental setups, and this approach will likely become more widespread in the context of research labs where novel devices or instruments are being developed.

Rapid prototyping: We believe that the greatest advantage of 3D printing lies with rapid prototyping. Novel devices which have intricate designs, including moving elements, embedded magnets, paper, electrodes or stir bars, and fluidic channels, have been demonstrated. Such developments would not have been possible without 3D printing, and it is likely that this will lead to further innovations for MS. We also expect more examples of full device integration where multi-material printing is used to combine sample preparation modules with an MS interface. One of the driving forces behind these developments is the complexity of devices that can be achieved in a single part, which simply cannot be matched by any other fabrication method.

Sharing and open-access: While there is great diversity in MS technology and 3D printing technology, the CAD process and data formats used for printing (namely *stl) are uniform. As a result, it is very easy, and increasingly common, to share designs as

supplementary information to a research paper. This could result in dedicated repositories where designs can simply be downloaded by a researcher, produced and used the very same day. Important in this discussion is the availability of 'adapters' that would allow the application of a device to different MS interfaces.

Improved fabrication: The increasing precision and reproducibility of 3D printing holds promise for the further improvement of the reproducibility of devices, such as the different extraction modules described in this work. This would mean that with time there will be more examples of analyses with improved detection limits. With improving precision, reproducibility and speed of 3D printing, we can expect on-demand commercial solutions for MS analysis executed with 3D printing. While currently there is a trade-off between printing speed and printing quality, new software and hardware innovations in additive manufacturing will decrease this trade-off, allowing one to fabricate macro-sized parts with sub-micrometer resolution in reasonable times. Since many of the described examples share their low-cost, lightweight, and integrative nature, the greatest promise for the implementation of 3D printing for MS lies perhaps in moving away from the laboratory setting to the site of sample collection.

Improved and functional materials: There are numerous materials and printing processes available for developing different applications. Future developments will likely result in easily printable materials with high chemical resistance and surface coatings and/or surface modifications that can be used to increase device functionality (e.g. 3D-printed SPE sorbents with different selectivities for diverse analytes). To date, a number of interesting functional materials have already been used, such as conductive or porous polymers. There are different functional materials commercially available, such as polymers with magnetic properties, that can be envisioned to appear in MS applications.

Implementation: Finally, the fact that 3D printing is referred to as a rapid prototyping technology suggests that after the prototyping stage, parts can and will be made in a more robust manner, from a material with superior properties. While this is probably true for fairly simple geometries that require an inert material, many of the applications shown in this review will not necessarily travel down this same road. For example, the aspect of open-science and instant sharing of designs is only applicable if combined with 3D printing. Moreover, when functional materials, such as porous sorbents or conductive plastic parts are produced, these have properties that make them indispensable. Finally, 3D printing, especially multi-material printing, allows the integration of the production and assembly processes into a single step, thereby improving the ease with which devices and elements can be produced and accurately aligned. Although initially used by hobbyists, 3D printing has become an indispensable tool in the arsenal of the analytical chemist, and we can look forward to seeing many MS-related improvements as a result.

CRediT authorship contribution statement

M. Grajewski: Conceptualization, Writing - original draft. **M. Hermann:** Conceptualization, Writing - original draft. **R.D. Oleschuk:** Conceptualization, Visualization, Writing - review & editing. **E. Verpoorte:** Conceptualization, Writing - review & editing. **G.IJ. Salentijn:** Conceptualization, Writing - original draft, Visualization, Writing - review & editing.

Declaration of competing interest

The authors declare that they have no known competing financial interests or personal relationships that could have appeared to influence the work reported in this paper.

Acknowledgements

E.V. and M.G. acknowledge financial support by the European Union Horizon 2020 Future and Emerging Technologies Programme (TISuMR project, grant number737043).

References

[1] D.T. Snyder, C.J. Pulliam, Z. Ouyang, R.G. Cooks, Miniature and fieldable mass spectrometers: recent advances, Anal. Chem. 88 (2016) 2–29, https://doi.org/10.1021/acs.analchem.5b03070.
[2] M.J.S. Symp, Bioprocessing - No longer a field of dreams, Macromol. Symp. 201 (2003) 271–281, https://doi.org/10.1002/masy.200351130.
[3] B.R.E. Drumright, P.R. Gruber, D.E. Henton, Polylactic acid technology, Adv. Mater. 12 (2000) 1841–1846.
[4] J.R. Dorgan, H.J. Lehermeier, L.-I. Palade, J. Cicero, Polylactides: properties and prospects of an environmentally benign plastic from renewable resources, Macromol. Symp. 175 (2001) 55–66.
[5] D. da Silva, M. Kaduri, M. Poley, O. Adir, N. Krinsky, J. Shainsky-Roitman, A. Schroeder, Biocompatibility, biodegradation and excretion of polylactic acid (PLA) in medical implants and theranostic systems, Chem. Eng. J. 340 (2018) 9–14, https://doi.org/10.1016/j.cej.2018.01.010.
[6] M.V. Varma, B. Kandasubramanian, C. Eng, S.M. Ibrahim, 3D printed scaffolds for biomedical applications, Mater. Chem. Phys. 255 (2020) 1–18, https://doi.org/10.1016/j.matchemphys.2020.123642.
[7] K.A. Athanasiou, G.G. Niederauer, C.M. Agrawal, Sterilization, toxicity, biocompatibility and clinical applications of polylactic acid/polyglycolic acid copolymers, Biomaterials 17 (1996) 93–102.
[8] R.M. Rasal, D.E. Hirt, Toughness decrease of PLA-PHBHHx blend films upon surface-confined photopolymerization, J. Biomed. Mater. Res. (2008) 1079–1086, https://doi.org/10.1002/jbm.a.32009.
[9] M. Dong, S. Zhang, D. Gao, B. Chou, The study on polypropylene applied in fused deposition modeling, in: AIP Conf. Proc, 2019.
[10] E.H. Baran, H.Y. Erbil, Surface modification of 3D printed PLA objects by fused deposition modeling: a review, Colloids and Interfaces 3 (2019) 1–25, https://doi.org/10.3390/colloids3020043.
[11] S. Martinez-Jarquin, A. Moreno-Pedraza, H. Guillen-Alonso, R. Winkler, Template for 3D printing a low-temperature plasma probe, Anal. Chem. 88 (2016) 6976–6980, https://doi.org/10.1021/acs.analchem.6b01019.
[12] K.S. Erokhin, E.G. Gordeev, V.P. Ananikov, Revealing interactions of layered polymeric materials at solid-liquid interface for building solvent compatibility charts for 3D printing applications, Sci. Rep. 9 (2019) 1–14, https://doi.org/10.1038/s41598-019-56350-w.
[13] E.G. Gordeev, E.S. Degtyareva, V.P. Ananikov, Analysis of 3D printing possibilities for the development of practical applications in synthetic organic chemistry, Russ. Chem. Bull. Int. Ed. 65 (2016) 1637–1643.
[14] T.P.N.D. Edith, S. Jean-luc, Surface characteristics of PLA and PLGA films, Appl. Surf. Sci. 253 (2006) 2758–2764, https://doi.org/10.1016/j.apsusc.2006.05.047.
[15] L. Elviri, R. Foresti, A. Bianchera, M. Silvestri, R. Bettini, 3D-printed polylactic acid supports for enhanced ionization efficiency in desorption electrospray mass spectrometry analysis of liquid and gel samples, Talanta 155 (2016) 321–328, https://doi.org/10.1016/j.talanta.2016.05.010.
[16] S. Sato, D. Gondo, T. Wada, S. Kanehashi, K. Nagai, Effects of various liquid organic solvents on solvent-induced crystallization of amorphous poly (lactic acid) film, J. Appl. Polym. Sci. (2013) 1607–1617, https://doi.org/10.1002/app.38833.
[17] T. Casalini, F. Rossi, A. Castrovinci, G. Perale, A perspective on polylactic acid-based polymers use for nanoparticles synthesis and applications, Front. Bioeng. Biotechnol. 7 (2019) 1–16, https://doi.org/10.3389/fbioe.2019.00259.
[18] I.H. Šrámková, B. Horstkotte, J. Erben, J. Chvojka, F. Švec, P. Solich, D. Šatínský, 3D-Printed magnetic stirring cages for semidispersive extraction of bisphenols from water using polymer micro- and nanofibers, Anal. Chem. 92 (2020) 3964–3971, https://doi.org/10.1021/acs.analchem.9b05455.
[19] G.IJ. Salentijn, H.P. Permentier, E. Verpoorte, 3D-Printed paper spray ionization cartridge with fast wetting and continuous solvent supply features, Anal. Chem. 86 (2014) 11657–11665, https://doi.org/10.1021/ac502785j.
[20] A. Jonsson, R.R. Svejdal, N. Bøgelund, T.T.T.N. Nguyen, H. Flindt, J.P. Kutter, K.D. Rand, J.P. Lafleur, Thiol-ene monolithic pepsin microreactor with a 3D-printed interface for efficient UPLC-MS peptide mapping analyses, Anal. Chem. 89 (2017) 4573–4580, https://doi.org/10.1021/acs.analchem.6b05103.
[21] S. Hwang, E.I. Reyes, K. Moon, R.C. Rumpf, N.S. Kim, Thermo-mechanical characterization of metal/polymer composite filaments and printing parameter study for fused deposition modeling in the 3D printing process, J. Electron. Mater. 44 (2015) 771–777, https://doi.org/10.1007/s11664-014-3425-6.
[22] W. Wu, P. Geng, G. Li, D. Zhao, H. Zhang, J. Zhao, Influence of layer thickness and raster angle on the mechanical properties of 3D-printed PEEK and a comparative mechanical study between PEEK and ABS, Materials 8 (2015) 5834–5846, https://doi.org/10.3390/ma8095271.

[23] J.F. Rodriguez, J.P. Thomas, J.E. Renaud, Mechanical behavior of acrylonitrile butadiene styrene (ABS) fused deposition materials, Exp. Invest. Rapid Prototyp. J. 7 (2001) 148–158.
[24] A.R.T. Perez, D.A. Roberson, R.B. Wicker, Fracture surface analysis of 3D-printed tensile specimens of novel ABS-based materials, J. Fail. Anal. Prev. 14 (2014) 343–353, https://doi.org/10.1007/s11668-014-9803-9.
[25] S. Chen, J. Lu, J. Feng, 3D-Printable ABS blends with improved scratch resistance and balanced mechanical performance, Ind. Eng. Chem. Res. 57 (2018) 3923–3931, https://doi.org/10.1021/acs.iecr.7b05074.
[26] P. Azimi, D. Zhao, C. Pouzet, N.E. Crain, B. Stephens, Emissions of ultrafine particles and volatile organic compounds from commercially available desktop three-dimensional printers with multiple filaments, Environ. Sci. Technol. 50 (2016) 1260–1268, https://doi.org/10.1021/acs.est.5b04983.
[27] M.T. Farcas, W. McKinney, C. Qi, K.W. Mandler, L. Battelli, S.A. Friend, A.B. Stefaniak, M. Jackson, M. Orandle, A. Winn, M. Kashon, R.F. LeBouf, K.A. Russ, D.R. Hammond, D. Burns, A. Ranpara, T.A. Thomas, J. Matheson, Y. Qian, Pulmonary and systemic toxicity in rats following inhalation exposure of 3-D printer emissions from acrylonitrile butadiene styrene (ABS) filament, Inhal. Toxicol. 32 (2020) 403–418, https://doi.org/10.1080/08958378.2020.1834034.
[28] Z. Weng, J. Wang, T. Senthil, L. Wu, Mechanical and thermal properties of ABS/montmorillonite nanocomposites for fused deposition modeling 3D printing, Mater. Des. 102 (2016) 276–283, https://doi.org/10.1016/j.matdes.2016.04.045.
[29] P. Zur, A. Kolodziej, A. Baier, G. Kokot, Optimization of ABS 3D-printing method and parameters, Eur. J. Eng. Sci. Technol. 3 (2020) 44–51.
[30] C. Koch, L. Van Hulle, N. Rudolph, Investigation of mechanical anisotropy of the fused filament fabrication process via customized tool path generation, Addit. Manuf. 16 (2017) 138–145, https://doi.org/10.1016/j.addma.2017.06.003.
[31] B.M. Tymrak, M. Kreiger, J.M. Pearce, Mechanical properties of components fabricated with open-source 3-D printers under realistic environmental conditions, Mater. Des. 58 (2014) 242–246, https://doi.org/10.1016/j.matdes.2014.02.038.
[32] J.T. Cantrell, S. Rohde, D. Damiani, R. Gurnani, L. Disandro, J. Anton, A. Young, A. Jerez, D. Steinbach, C. Kroese, P.G. Ifju, Experimental characterization of the mechanical properties of 3D-printed ABS and polycarbonate parts, Rapid Prototyp. J. 23 (2017) 811–824, https://doi.org/10.1108/RPJ-03-2016-0042.
[33] E.J. Mccullough, V.K. Yadavalli, Surface modification of fused deposition modeling ABS to enable rapid prototyping of biomedical microdevices, J. Mater. Process. Technol. 213 (2013) 947–954, https://doi.org/10.1016/j.jmatprotec.2012.12.015.
[34] L.C. Duarte, T.C. De Carvalho, E.O. Lobo-Junior, P. V Abdelnur, B.G. Vaz, W.K.T. Coltro, 3D printing of microfluidic devices for paper-assisted direct spray ionization mass spectrometry, Anal. Methods. 8 (2016) 496–503, https://doi.org/10.1039/c5ay03074a.
[35] J. Hu, T. Chen, C. Chang, J. Cheng, Y. Chen, P.L. Urban, A compact 3D-printed interface for coupling open digital microchips with Venturi easy ambient sonic-spray ionization mass spectrometry, Analyst 140 (2015) 1495–1501, https://doi.org/10.1039/c4an02220c.
[36] E.M. Tridas, C. Allemang, F. Mast, J. Mark, R. Schlaf, High transmission 3D printed flex-PCB-based ion funnel, J. Mass Spectrom. 50 (2015) 938–943, https://doi.org/10.1002/jms.3606.
[37] K.J.M. Francisco, C.L. do Lago, A capillary electrophoresis system with dual capacitively coupled contactless conductivity detection and electrospray ionization tandem mass spectrometry, Electrophoresis 37 (2016) 1718–1724, https://doi.org/10.1002/elps.201600005.
[38] N. Kumar, P.K. Jain, P. Tandon, P. Mohan, Experimental investigations on suitability of polypropylene (PP) and ethylene vinyl acetate (EVA) in additive manufacturing, Mater. Today Proc. 5 (2018) 4118–4127, https://doi.org/10.1016/j.matpr.2017.11.672.
[39] G. Scotti, S.M.E. Nilsson, M. Haapala, P. Pöhö, G.B. af Gennas, J. Yli-kauhaluoma, T. Kotiaho, A miniaturised 3D printed polypropylene reactor for on-line reaction analysis by mass spectrometry, React. Chem. Eng. 2 (2017) 299–303, https://doi.org/10.1039/c7re00015d.
[40] M.R. Penny, Z.X. Rao, F. Peniche, S.T. Hilton, Modular 3D printed compressed air driven continuous-flow systems for chemical synthesis, Eur. J. Org Chem. (2019) 3783–3787, https://doi.org/10.1002/ejoc.201900423.
[41] J.S. Mathieson, M.H. Rosnes, V. Sans, P.J. Kitson, L. Cronin, Continuous parallel ESI-MS analysis of reactions carried out in a bespoke 3D printed device, Beilstein J. Nanotechnol. 4 (2013) 285–291, https://doi.org/10.3762/bjnano.4.31.
[42] M. Vaezi, S. Yang, Extrusion-based additive manufacturing of PEEK for biomedical applications, Virtual Phys. Prototyp. 10 (2015) 123–135, https://doi.org/10.1080/17452759.2015.1097053.
[43] Y. Li, Y. Lou, Tensile and bending strength improvements in PEEK parts using fused deposition modelling 3D printing considering multi-factor coupling, Polymers 12 (2020) 1–14.
[44] S. Najeeb, M.S. Zafar, Z. Khurshid, F. Siddiqui, Applications of polyetheretherketone (PEEK) in oral implantology and prosthodontics, J. Prosthodont. Res. 60 (2015) 12–19, https://doi.org/10.1016/j.jpor.2015.10.001.
[45] I.V. Panayotov, V. Orti, F. Cuisinier, J. Yachouh, Polyetheretherketone (PEEK) for medical applications, J. Mater. Sci. Mater. Med. 27 (2016) 1–11, https://doi.org/10.1007/s10856-016-5731-4.
[46] L. Bathala, V. Majeti, N. Rachuri, N. Singh, S. Gedela, The role of polyether ether ketone (PEEK) in dentistry – a review, J. Med. Life. 12 (2019) 5–9, https://doi.org/10.25122/jml-2019-0003.
[47] S.M. Kurtz, J.N. Devine, PEEK biomaterials in trauma, orthopedic, and spinal implants, Biomaterials 28 (2007) 4845–4869, https://doi.org/10.1016/j.biomaterials.2007.07.013.
[48] B. Valentan, Z. Kadivnik, T. Brajlih, A. Anderson, I. Drstvensek, Processing Poly(ether etherketone) on a 3D printer for thermoplastic modelling, Mater. Technol. 47 (2013) 715–721.
[49] K.H. Tan, C.K. Chua, K.F. Leong, C.M. Cheah, P. Cheang, M.S.A. Bakar, S.W. Cha, Scaffold development using selective laser sintering of polyetheretherketone – hydroxyapatite biocomposite blends, Biomaterials 24 (2003) 3115–3123, https://doi.org/10.1016/S0142-9612(03)00131-5.
[50] M. Schmidt, D. Pohle, T. Rechtenwald, Selective laser sintering of PEEK, Ann. CIRP. 56 (2007) 205–208, https://doi.org/10.1016/j.cirp.2007.05.097.
[51] B.C. Hauck, B.R. Ruprecht, P.C. Riley, L.D. Strauch III, Reproducible 3D-printed unibody drift tubes for ion mobility spectrometry, Sensor. Actuator. B Chem. 323 (2020) 1–6, https://doi.org/10.1016/j.snb.2020.128671.
[52] A. Hollerbach, Z. Baird, R.G. Cooks, Ion separation in air using a three-dimensional printed ion mobility spectrometer, Anal. Chem. 89 (2017) 5058–5065, https://doi.org/10.1021/acs.analchem.7b00469.
[53] A. Hollerbach, P.W. Fedick, R.G. Cooks, Ion Mobility–Mass spectrometry using a dual-gated 3D printed ion mobility spectrometer, Anal. Chem. 90 (2018) 13265–13272.
[54] K. Iyer, B.M. Marsh, G.O. Capek, R.L. Schrader, S. Tichy, R.G. Cooks, Ion manipulation in open air using 3D-printed electrodes, J. Am. Soc. Mass Spectrom. 30 (2019) 2584–2593, https://doi.org/10.1021/jasms.8b06275.
[55] R.L. Schrader, B.M. Marsh, R.G. Cooks, Temporal distribution of ions in ambient pressure drift tubes with turns, Int. J. Mass Spectrom. 456 (2020) 1–6, https://doi.org/10.1016/j.ijms.2020.116391.
[56] C. Su, J. Lin, 3D-Printed column with porous monolithic packing for online solid-phase extraction of multiple trace metals in environmental water samples, Anal. Chem. 92 (2020) 9640–9648, https://doi.org/10.1021/acs.analchem.0c00863.
[57] U. Kalsoom, C.K. Hasan, L. Tedone, C. Desire, F. Li, M.C. Breadmore, P.N. Nesterenko, B. Paull, Low-cost passive sampling device with integrated porous membrane produced using multimaterial 3D printing, Anal. Chem. 90 (2018) 12081–12089, https://doi.org/10.1021/acs.analchem.8b02893.
[58] L. Konieczna, M. Belka, M. Oko, M. Pyszka, T. Baczek, New 3D-printed sorbent for extraction of steroids from human plasma preceding LC–MS analysis, J. Chromatogr., A 1545 (2018) 1–11, https://doi.org/10.1016/j.chroma.2018.02.040.
[59] D. Wang, X. Huang, J. Li, B. He, Q. Liu, L. Hu, G. Jiang, 3D printing of graphene-doped target for 'matrix-free' laser desorption/ionization mass spectrometry, Chem. Commun. 54 (2018) 2723–2726, https://doi.org/10.1039/c7cc09649f.
[60] J. Fialova, J. Hrabak, V. Studentova, D. Kavan, P. Pompach, P. Novak, Three-dimensional printed target plates for matrix-assisted laser desorption/ionization mass spectrometry, Anal. Chem. 92 (2020) 12783–12788, https://doi.org/10.1021/acs.analchem.0c01737.
[61] D. Wang, B. He, X. Yan, Q. Nong, C. Wang, J. Jiang, L. Hu, G. Jiang, 3D printed gel electrophoresis device coupling with ICP-MS for online separation and detection of metalloproteins, Talanta 197 (2019) 145–150, https://doi.org/10.1016/j.talanta.2019.01.025.
[62] P. Sosnowski, G. Hopfgartner, Application of 3D printed tools for customized open port probe-electrospray mass spectrometry, Talanta 215 (2020) 1–8, https://doi.org/10.1016/j.talanta.2020.120894.
[63] V. Garcia-montoto, S. Mallet, C. Arnaudguilhem, J.H. Christensen, B. Bouyssiere, 3D-printed total consumption microflow nebuliser development for trace element analysis in organic matrices via inductively coupled plasma mass spectrometry, J. Anal. At. Spectrom. 35 (2020) 1552–1557, https://doi.org/10.1039/d0ja00182a.
[64] N.P. Macdonald, J.M. Cabot, P. Smejkal, R.M. Guijt, B. Paull, M.C. Breadmore, Comparing microfluidic performance of three-dimensional (3D) printing platforms, Anal. Chem. 89 (2017) 3858–3866, https://doi.org/10.1021/acs.analchem.7b00136.
[65] N.P. MacDonald, F. Zhu, C.J. Hall, J. Reboud, P.S. Crosier, E.E. Patton, D. Wlodkowic, J.M. Cooper, Assessment of biocompatibility of 3D printed photopolymers using zebrafish embryo toxicity assays, Lab Chip 16 (2016) 291–297, https://doi.org/10.1039/c5lc01374g.
[66] F. Fina, A. Goyanes, S. Gaisford, A.W. Basit, Selective laser sintering (SLS) 3D printing of medicines, Int. J. Pharm. 529 (2017) 285–293, https://doi.org/10.1016/j.ijpharm.2017.06.082.
[67] F. Kotz, K. Arnold, W. Bauer, D. Schild, N. Keller, K. Sachsenheimer, T.M. Nargang, C. Richter, D. Helmer, B.E. Rapp, Three-dimensional printing of transparent fused silica glass, Nature 544 (2017) 337–339, https://doi.org/10.1038/nature22061.
[68] B. Gross, S.Y. Lockwood, D.M. Spence, Recent advances in analytical chemistry by 3D printing, Anal. Chem. 89 (2017) 57–70, https://doi.org/10.1021/acs.analchem.6b04344.
[69] R. Walczak, K. Adamski, Inkjet 3D printing of microfluidic structures - on the selection of the printer towards printing your own microfluidic chips, J. Micromech. Microeng. 25 (2015) 1–11, https://doi.org/10.1088/0960-1317/25/8/085013.
[70] M.J. Jacobs, C.W. Pinger, A.D. Castiaux, K.J. Maloney, D.M. Spence, A novel 3D-printed centrifugal ultrafiltration method reveals in vivo glycation of human

serum albumin decreases its binding affinity for zinc, Metall 12 (2020) 1036–1043, https://doi.org/10.1039/d0mt00123f.
[71] S. Kulomäki, E. Lahtinen, S. Perämäki, A. Väisänen, Determination of mercury at picogram level in natural waters with inductively coupled plasma mass spectrometry by using 3D printed metal scavengers, Anal. Chim. Acta 1092 (2019) 24–31, https://doi.org/10.1016/j.aca.2019.09.075.
[72] H. Wang, D.J. Cocovi-Solberg, B. Hu, M. Miro, 3D-Printed micro flow injection analysis platform for online magnetic nanoparticle sorptive extraction of antimicrobials in biological specimens as a front end to liquid chromatographic assays, Anal. Chem. (2017) 12541–12549, https://doi.org/10.1021/acs.analchem.7b03767.
[73] D.A.V. Medina, Á.J. Santos-Neto, V. Cerdà, F. Maya, Automated dispersive liquid-liquid microextraction based on the solidification of the organic phase, Talanta 189 (2018) 241–248, https://doi.org/10.1016/j.talanta.2018.06.081.
[74] R.M. Frizzarin, C.P. Cabello, M. del M. Bauzà, L.A. Portugal, F. Maya, V. Cerdà, J.M. Estela, G.T. Palomino, Submicrometric magnetic nanoporous carbons derived from metal-organic frameworks enabling automated electromagnet-assisted online solid-phase extraction, Anal. Chem. 88 (2016) 6990–6995, https://doi.org/10.1021/acs.analchem.6b02065.
[75] É.M. Kataoka, R.C. Murer, J.M. Santos, R.M. Carvalho, M.N. Eberlin, F. Augusto, R.J. Poppi, A.L. Gobbi, L.W. Hantao, Simple, expendable, 3D-printed microfluidic systems for sample preparation of petroleum, Anal. Chem. 89 (2017) 3460–3467, https://doi.org/10.1021/acs.analchem.6b04413.
[76] A. Dominguez-tello, A. Dominguez-alfaro, J.L. Gómez-ariza, A. Arias-borrego, T. Garcia-Barrera, Effervescence-assisted spiral hollow-fibre liquid-phase microextraction of trihalomethanes, halonitromethanes, haloacetonitriles, and haloketones in drinking water, J. Hazard Mater. 397 (2020) 1–12, https://doi.org/10.1016/j.jhazmat.2020.122790.
[77] X. Huang, D. Wang, B. He, Q. Liu, L. Hu, G. Jiang, A 3D-printed modularized purification system for rapid, high-throughput MALDI-MS analysis of small-volume biological samples, Chem. Commun. 56 (2020) 1637–1640, https://doi.org/10.1039/c9cc08832f.
[78] M. Wang, P. Laborda, L.P. Conway, X. Duan, K. Huang, L. Liu, J. Voglmeir, An integrated 3D-printed platform for the automated isolation of N-glycans, Carbohydr. Res. 433 (2016) 14–17, https://doi.org/10.1016/j.carres.2016.06.007.
[79] D.J. Harney, A.T. Hutchison, L. Hatchwell, S.J. Humphrey, D.E. James, S. Hocking, L.K. Heilbronn, M. Larance, Proteomic analysis of human plasma during intermittent fasting, J. Proteome Res. 18 (2019) 2228–2240, https://doi.org/10.1021/acs.jproteome.9b00090.
[80] G. Scotti, M.E. Nilsson, V. Matilainen, M. Haapala, G.B. af Gennas, J. Yli-kauhaluoma, A. Salminen, T. Kotiaho, Simple 3D printed stainless steel microreactors for online mass spectrometric analysis, Heliyon 5 (2019), https://doi.org/10.1016/j.heliyon.2019.e02002, 1-7.
[81] M. Tascon, V. Singh, M. Huq, J. Pawliszyn, Direct coupling of dispersive extractions with magnetic particles to mass spectrometry via microfluidic open interface, Anal. Chem. 91 (2019) 4762–4770, https://doi.org/10.1021/acs.analchem.9b00308.
[82] C.K. Su, Y.T. Chen, Y.C. Sun, Speciation of trace iron in environmental water using 3D-printed minicolumns coupled with inductively coupled plasma mass spectrometry, Microchem. J. 146 (2019) 835–841, https://doi.org/10.1016/j.microc.2019.02.015.
[83] T.T. Häbe, G.E. Morlock, Open-source add-on kit for automation of zone elution in planar chromatography, Rapid Commun. Mass Spectrom. 34 (2020) 1–9, https://doi.org/10.1002/rcm.8631.
[84] G.IJ. Salentijn, P.E. Oomen, M. Grajewski, E. Verpoorte, Fused deposition modeling 3D printing for (Bio)analytical device fabrication: procedures, materials, and applications, Anal. Chem. 89 (2017) 7053–7061, https://doi.org/10.1021/acs.analchem.7b00828.
[85] C.L. Feider, A. Krieger, R.J. Dehoog, L.S. Eberlin, Ambient ionization mass spectrometry: recent developments and applications, Anal. Chem. 91 (2019) 4266–4290, https://doi.org/10.1021/acs.analchem.9b00807.
[86] Z. Takáts, J.M. Wiseman, B. Gologan, R.G. Cooks, Mass spectrometry sampling under ambient conditions with desorption electrospray ionization, Science 306 (2004) 471–473, https://doi.org/10.1126/science.1104404.
[87] R.B. Cody, J.A. Larame, H.D. Durst, Versatile new ion source for the analysis of materials in open air under ambient conditions, Anal. Chem. 77 (2005) 2297–2302, https://doi.org/10.1021/ac050162j.
[88] J. Liu, H. Wang, N.E. Manicke, J. Lin, R.G. Cooks, Development, characterization, and application of paper spray ionization, Anal. Chem. 82 (2010) 2463–2471, https://doi.org/10.1021/ac902854g.
[89] Q. Yang, H. Wang, J.D. Maas, W.J. Chappell, N.E. Manicke, R.G. Cooks, Z. Ouyang, Paper spray ionization devices for direct, biomedical analysis using mass spectrometry, Int. J. Mass Spectrom. 312 (2012) 201–207, https://doi.org/10.1016/j.ijms.2011.05.013.
[90] G.IJ. Salentijn, R.D. Oleschuk, E. Verpoorte, 3D-Printed paper spray ionization cartridge with integrated desolvation feature and ion optics, Anal. Chem. 89 (2017) 11419–11426, https://doi.org/10.1021/acs.analchem.7b02490.
[91] B.J. Bills, J. Kinkade, G. Ren, N.E. Manicke, The impacts of paper properties on matrix effects during paper spray mass spectrometry analysis of prescription drugs, fentanyl and synthetic cannabinoids, Forensic Chem 11 (2018) 15–22, https://doi.org/10.1016/j.forc.2018.08.002.
[92] C. Zhang, T. Glaros, N.E. Manicke, Targeted protein detection using an all-in-one mass spectrometry cartridge, J. Am. Chem. Soc. 139 (2017) 10996–10999, https://doi.org/10.1021/jacs.7b05571.
[93] Y. Yang, H. Liu, Z. Chen, T. Wu, Z. Jiang, L. Tong, B. Tang, A simple 3D-printed enzyme reactor paper spray mass spectrometry platform for detecting BuChE activity in human serum, Anal. Chem. 91 (2019) 12874–12881, https://doi.org/10.1021/acs.analchem.9b02728.
[94] E.S. Dhummakupt, P.M. Mach, D. Carmany, P.S. Demond, T.S. Moran, T. Connell, H.S. Wylie, N.E. Manicke, J.M. Nilles, T. Glaros, Direct analysis of aerosolized chemical warfare simulants captured on a modified glass-based substrate by “paper-spray” ionization, Anal. Chem. 89 (2017) 10866–10872, https://doi.org/10.1021/acs.analchem.7b02530.
[95] S. Martinez-Jarquin, A. Moreno-Pedraza, D. Carzarez-Garcia, R. Winkler, Automated chemical fingerprinting of Mexican spirits derived from Agave (tequila and mezcal) using direct-injection electrospray ionisation (DIESI) and low-temperature plasma (LTP) mass spectrometry, Anal. Methods. 9 (2017) 5023–5028, https://doi.org/10.1039/c7ay00793k.
[96] A. Moreno-Pedraza, I. Rosas-Román, N.S. Garcia-Rojas, H. Guillén-Alonso, C. Ovando-Vázquez, D. Díaz-Ramírez, J. Cuevas-Contreras, F. Vergara, N. Marsch-Martínez, J. Molina-Torres, R. Winkler, Elucidating the distribution of plant metabolites from native tissues with laser desorption low-temperature plasma mass spectrometry imaging, Anal. Chem. 91 (2019) 2734–2743, https://doi.org/10.1021/acs.analchem.8b04406.
[97] E.D. Hoegg, T.J. Williams, D.W. Koppenaal, J.R. Bills, R.K. Marcus, D.W. Koppenaal, A multi-electrode glow discharge ionization source for atomic and molecular mass spectrometry, J. Anal. At. Spectrom. 35 (2020) 1969–1978, https://doi.org/10.1039/d0ja00142b.
[98] C.J. Pulliam, R.M. Bain, H.L. Osswald, D.T. Snyder, P.W. Fedick, S.T. Ayrton, T.G. Flick, R.G. Cooks, Simultaneous online monitoring of multiple reactions using a miniature mass spectrometer, Anal. Chem. 89 (2017) 6969–6975, https://doi.org/10.1021/acs.analchem.7b00119.
[99] K.J. Zemaitis, T.D. Wood, Integration of 3D-printing for a desorption electrospray ionization source for mass spectrometry, Rev. Sci. Instrum. 91 (2020) 1–7, https://doi.org/10.1063/5.0004626.
[100] B.E. Draper, S.N. Anthony, M.F. Jarrold, The FUNPET — a new hybrid ion funnel-ion carpet atmospheric pressure interface for the simultaneous transmission of a broad mass range, J. Am. Soc. Mass Spectrom. 29 (2018) 2160–2172, https://doi.org/10.1021/jasms.8b05708.
[101] R.L. Schrader, B.M. Marsh, R.G. Cooks, Fourier transform-ion mobility linear ion trap mass spectrometer using frequency encoding for recognition of related compounds in a single acquisition, Anal. Chem. 92 (2020) 5107–5115, https://doi.org/10.1021/acs.analchem.9b05507.
[102] C.J. Pulliam, R.M. Bain, H.L. Osswald, D.T. Snyder, P.W. Fedick, S.T. Ayrton, T.G. Flick, R.G. Cooks, Simultaneous online monitoring of multiple reactions using a miniature mass spectrometer, Anal. Chem. 89 (2017) 6969–6975, https://doi.org/10.1021/acs.analchem.7b00119.
[103] K.J.M. Francisco, C.L. do Lago, Improving thermal control of capillary electrophoresis with mass spectrometry and capacitively coupled contactless conductivity detection by using 3D printed cartridges, Talanta 185 (2018) 37–41, https://doi.org/10.1016/j.talanta.2018.03.052.
[104] C. Liu, K. Choi, Y. Kang, J. Kim, C. Fobel, B. Seale, J.L. Campbell, T.R. Covey, A.R. Wheeler, Direct interface between digital microfluidics and high performance liquid chromatography-mass spectrometry, Anal. Chem. 87 (2015) 11967–11972, https://doi.org/10.1021/acs.analchem.5b03616.
[105] A. Jonsson, J.P. Lafleur, D. Sticker, J.P. Kutter, An all thiol-ene microchip for solid phase extraction featuring an in situ polymerized monolith and integrated 3D replica-molded emitter for direct electrospray mass spectrometry, Anal. Methods. 10 (2018) 2854–2862, https://doi.org/10.1039/c8ay00646f.
[106] E.P. Dutkiewicz, H.Y. Chiu, P.L. Urban, Micropatch-arrayed pads for non-invasive spatial and temporal profiling of topical drugs on skin surface, J. Mass Spectrom. 50 (2015) 1321–1325, https://doi.org/10.1002/jms.3702.
[107] A. Tycova, J. Prikryl, F. Foret, Reproducible preparation of nanospray tips for capillary electrophoresis coupled to mass spectrometry using 3D printed grinding device, Electrophoresis 37 (2016) 924–930, https://doi.org/10.1002/elps.201500467.